

Redundant functions of miR156-targeted SQUAMOSA PROMOTER BINDING PROTEIN-LIKE transcription factors in promoting cauline leaf identity

Darren Manuela¹ , Liren Du¹ , Qi Zhang¹, Yifei Liao¹ , Tieqiang Hu¹ , Jim P. Fouracre²  and Mingli Xu¹ 

¹Department of Biological Sciences, University of South Carolina, Columbia, SC 29208, USA; ²School of Biological Sciences, University of Bristol, Bristol, BS8 1TQ, UK

Summary

Author for correspondence:

Mingli Xu

Email: minglixu@sc.edu

Received: 9 December 2024

Accepted: 21 April 2025

New Phytologist (2025) **247**: 719–737

doi: 10.1111/nph.70210

Key words: BR11, cauline leaf, FUL, SOC1, SPL.

- Cauline leaf development represents an intermediate phase between vegetative and reproductive stages. While extensive research has been conducted on the genetic and environmental factors that determine cauline leaf number, less attention has been given to the regulation of their morphology and the establishment of cauline leaf identity.
- In this study, we report that miR156-targeted SQUAMOSA PROMOTER BINDING PROTEIN-LIKE (SPL) transcription factors, including SPL2, SPL9, SPL10, SPL11, SPL13, and SPL15, redundantly regulate cauline leaf identity, affecting both cauline leaf shape and the number of leaves on secondary inflorescences. This function is distinct from that of floral meristem identity genes, which affect the number of cauline leaves by promoting floral fate.
- We further show that the inducers of reproductive development SUPPRESSOR OF OVER-EXPRESSION OF CONSTANS1 (SOC1) and FRUITFUL (FUL) directly bind to and activate *SPL9* and *SPL15*, linking floral induction pathways to the regulation of cauline leaf identity. Additionally, we demonstrate that the brassinosteroid receptor BRASSINOSTEROID INSENSITIVE 1 (*BRI1*) is co-expressed with miR156-targeted *SPLs* in cauline leaves and is a direct target of *SPL9*.
- Together, this study uncovers a SOC1/FUL-SPL-BRI1 module that governs cauline leaf identity, providing new insights into the regulatory networks that control plant inflorescence architecture.

Introduction

Shoot development in flowering plants is characterized by two phases: a vegetative phase, during which leaves are produced, and a reproductive phase, when plants produce flowers. The vegetative phase can be further divided into the juvenile and adult stages, which, depending on the species, can often be distinguished by changes in leaf morphology. The transition from the juvenile to adult vegetative stage, known as vegetative phase change, is regulated by two closely related microRNAs, miR156 and miR157, and their direct targets in the SQUAMOSA PROMOTER BINDING PROTEIN-LIKE (SPL) family of transcription factors, which promote developmental traits in adult plants (Wu *et al.*, 2009; Xu *et al.*, 2016; He *et al.*, 2018; Poethig & Fouracre, 2024). In all surveyed flowering plants, miR156/miR157 are highly expressed during early vegetative development but decrease in expression as a shoot ages, leading to the de-repression of SPL activity and the transition to adult growth. In *Arabidopsis*, juvenile leaves exhibit small rounded blades with smooth margins, the absence of abaxial trichomes, and distinctly delimited elongated petioles, whereas adult leaves

are longer, serrated, produce abaxial trichomes, and have a less distinct petiole (Xu *et al.*, 2016; He *et al.*, 2018). Ten members of the SPL family are targeted by miR156/157 in *Arabidopsis*, of which *SPL2*, *SPL9*, *SPL10*, *SPL11*, *SPL13*, and *SPL15* have the largest effect on leaf development (Xu *et al.*, 2016; Hu *et al.*, 2023).

During the reproductive phase, the vegetative shoot apical meristem (SAM) is transformed into an inflorescence meristem (IM; Ratcliffe *et al.*, 1998) and flowers are produced instead of leaves on the lateral flanks of the meristem. Cauline leaves are formed during an intermediate phase between vegetative and reproductive development, in that they initiate during vegetative development but convert to cauline identity following floral induction (Hempel *et al.*, 1997). They represent the end state of the heteroblastic process of leaf development in *Arabidopsis*, as they lack petioles and have long, narrow lamina, and trichomes are predominantly produced on the abaxial surface (Yang & Jiao, 2016). Unlike juvenile or adult leaves, which contribute to the flat rosette habit of *Arabidopsis*, cauline leaves form on the aerial stem and are associated with elongated internodes. Previous work has suggested that a subset of *SPL* genes regulate cauline leaf

morphology as well as that of rosette leaves (Shikata *et al.*, 2009), although the generality of this regulatory interaction and its mechanistic basis have yet to be investigated.

Typically, wild-type (WT) plants produce three to four cauline leaves in long-day (LD) conditions on the primary inflorescence stem, with each subsequent cauline leaf becoming narrower and having fewer adaxial trichomes than the previous one (Telfer *et al.*, 1997). As with vegetative leaves, cauline leaves also subtend axillary meristems. The outgrowth of the axillary meristems of cauline leaves on the primary inflorescence iteratively produces secondary inflorescence branches, which further initiate cauline leaves, elongated internodes, and eventually, flowers (Supporting Information Fig. S1a; Yang & Jiao, 2016). Cauline leaves have wide-ranging roles during plant growth, including the protection of emerging inflorescences, drought and pathogen defense, and active photosynthesis (Pabón-Mora *et al.*, 2013; Patharkar & Walker, 2016; Patharkar *et al.*, 2017; Aryal *et al.*, 2018; Patharkar, 2019; Ding *et al.*, 2023); it is therefore important to understand the molecular mechanisms that govern cauline identity.

Floral induction is a key step in cauline leaf identity, as evidenced by the fact that plants transferred from noninductive short-day (SD) conditions to inductive LD conditions form cauline leaves several days after transfer, while plants that remain in SD conditions continue to produce vegetative leaves at the same time (Hempel *et al.*, 1997; Torti *et al.*, 2012). Floral induction is regulated by the interaction between the photoperiod, vernalization, gibberellic acid, thermosensory, age-dependent, and autonomous pathways, and is ultimately dependent on the upregulation of the key floral integrators FLOWERING LOCUS T (FT) and MADS-box transcription factor SUPPRESSOR OF OVEREXPRESSION OF CONSTANS1 (SOC1; Lee & Lee, 2010; Cho *et al.*, 2017; Freytes *et al.*, 2021). The upregulation of *FT* and *SOC1* promotes the transition from vegetative SAM to IM fate and correlates with the conversion of vegetative leaves to cauline identity (Ratcliffe *et al.*, 1998; Borner *et al.*, 2000). Closely related SOC1-like MADS-box transcription factors, such as AGAMOUS-like24 (AGL24), AGL42, and FRUITFUL (FUL), as well as the zinc-finger transcription factor CONSTANS (CO) and the bZIP transcription factor FD, also promote floral induction in part with SOC1 (Samach *et al.*, 2000; Wigge *et al.*, 2005; Liu *et al.*, 2008; Torti & Fornara, 2012; Balanzà *et al.*, 2014). In addition, several SPLs directly promote *SOC1* and *FUL*, although recent work suggests that SPLs do not have a functionally significant role in floral induction in *Arabidopsis* (Shikata *et al.*, 2009; Wang *et al.*, 2009; Doody *et al.*, 2022; Zhao *et al.*, 2023). After being activated, SOC1 directly promotes the expression of the master floral meristem identity gene *LEAFY* (*LFY*). *LEAFY* upregulates the expression of *APETALA1* (*API*), and together, they promote the initiation of floral meristems (Weigel *et al.*, 1992; Blázquez *et al.*, 1997; Busch *et al.*, 1999; Wagner *et al.*, 1999).

Although there has been much focus on elucidating the genetic networks that regulate vegetative leaf identity and floral induction, whether these networks interact to establish cauline leaf identity has been largely overlooked. Here, we demonstrate that, similar to vegetative leaves, cauline leaf identity is regulated by

the miR156-SPL pathway. We further show that *SPL* genes function directly downstream of the floral inducers SOC1 and FUL to promote cauline leaf development and identify a novel interaction between SPL transcription factors and the brassinosteroid (BR) receptor BRASSINOSTEROID INSENSITIVE 1 (BRI1). Taken together, our results reveal that cauline leaf identity is regulated in part by a SOC1/FUL-SPL-BRI1 genetic module.

Materials and Methods

Plant material and growth conditions

Seeds were sown on Sunshine SS#8F2 potting soil, stratified at 4°C for 2–4 d, and transferred to Conviron growth chambers. Plants were grown at a constant 22°C under LD conditions (16 h : 8 h, light : dark; 95 $\mu\text{mol m}^{-2} \text{s}^{-1}$ irradiance). Plants induced to flower by transfer to LD conditions were first grown for 2 wk under SD conditions (10 h : 14 h, light : dark; 120 $\mu\text{mol m}^{-2} \text{s}^{-1}$ irradiance). *Arabidopsis* plants in the Columbia (Col-0) ecotype were used in this study. *soc1-2* (Lee *et al.*, 2008), *ful-2* (Balanzà *et al.*, 2014), *agl24-3* (SALK_095007), *co-10* (CS2109735), *fd-3* (SALK_054421C), and *lfy-1* (CS6228) were obtained from the Arabidopsis Biological Resource Center (Ohio State University, Columbus, OH, USA). *spl2-1* (SALK_022235), *spl9-4* (SAIL_150_B05), *spl10* (Xu *et al.*, 2016), *spl11-1* (FLAG_422H07), *spl13-1* (Xu *et al.*, 2016), and *spl15-1* (SALK_074426) were gifts from Dr Scott Poethig, and *co-10* (CS2109735) and *fd-3* (SALK_054421C) were gifts from Dr George Coupland. The *agl42* mutant line was generated by CRISPR-cas9 by the guide RNA (5'-CTC CAA AGA AGT CTG GGA A-3') using a previously described protocol (Xing *et al.*, 2014; Fig. S2). *bri1-301* and *bri1-116* were gifts from Dr Jia Li. Higher order mutants were made by crossing, and homozygous F2 generation lines were isolated using allele-specific primers for genotyping listed in Table S1.

Transgenic plants

The *SPL2:SPL2-GUS*, *SPL9:SPL9-GUS*, *SPL10:SPL10-GUS*, *SPL11:SPL11-GUS*, *SPL13:SPL13-GUS*, *SPL15:SPL15-GUS*, and *35S:MIM156* lines were described previously (Xu *et al.*, 2016). The *35S:SOC1* and *35S:CO* lines were gifts from Dr George Coupland, and *35S:FUL* was a gift from Dr Marian Bemer. *35S:AGL24*, *35S:AGL42*, and *35S:FD* lines were constructed using the Golden Gate system (Weber *et al.*, 2011). The *AGL24* cDNA, *AGL42* cDNA, and *FD* cDNA were cloned using the primers listed in Table S2. The cauliflower mosaic virus 35S promoter was fused to the 5' end of these cDNA fragments, and constructs were transformed into Col-0 by floral dipping (Clough & Bent, 1998). The *SOC1:GUS*, *FUL:GUS*, *AGL24:GUS*, and *FD:GUS* lines were described previously as well (Fouracre & Poethig, 2019; Manuela & Xu, 2024). The *CO:GUS* and *AGL42:GUS* lines were constructed using the Golden Gate system (Weber *et al.*, 2011). The promoters of *CO* (3180 bp) and *AGL42* (2479 bp) were cloned using the primers listed in Table S2, and the bacterial β -glucuronidase (GUS) cDNA was

fused to the 3' end of these promoter fragments. These constructs were transformed into Col-0 by floral dipping. The *FD:MIR156A* line was described previously (Fouracre & Poethig, 2019). The *SOC1:MIR156A*, *FUL:MIR156A*, *CO:MIR156A*, *AGL24:MIR156A*, and *AGL42:MIR156A* lines were constructed using the Golden Gate system (Weber *et al.*, 2011), and the promoters of *SOC1* (4046 bp), *FUL* (5190 bp), *CO* (3180 bp), *AGL24* (2234 bp), and *AGL42* (2479 bp), and *MIR156A* cDNA were cloned using the primers listed in Table S2. The *MIR156A* cDNA was fused to the 3' end of these promoter fragments, and these constructs were transformed into Col-0 by floral dipping (Clough & Bent, 1998).

The *proSOC1:SOC1-GFP* line was constructed using the Golden Gate system as well (Weber *et al.*, 2011). The *SOC1* cDNA excluding the stop codon was cloned using the primers listed in Table S2. The same 4046-bp *SOC1* promoter used previously was fused to the 5' end of this *SOC1* cDNA, and a green fluorescent protein (GFP) tag was fused to the 3' end. This construct was transformed into the *soc1-2* mutant by floral dipping, and the lines that complemented these mutants were selected for chromatin immunoprecipitation followed by qPCR (ChIP-qPCR; Clough & Bent, 1998). *35S:FUL-GFP* and *SPL9:GFP-rSPL9 spl9/13 (rSpl9)* were constructed similarly and have been described previously (Hu *et al.*, 2023; Manuela & Xu, 2024). The *proSPL9:SPL9gDNA-GUS (SPL9:SPL9-GUS)* and *proSPL9trunc:SPL9gDNA-GUS (SPL9trunc:SPL9-GUS)* lines were also constructed using the Golden Gate system (Weber *et al.*, 2011). The *SPL9* promoter (3387 bp), a truncated *SPL9* promoter (2982 bp), and *SPL9* gDNA without the stop codon were cloned using the primers listed in Table S2. The *SPL9* promoter and truncated *SPL9* promoter were then fused to the 5' end of the *SPL9* gDNA, and the *GUS* cDNA was fused to the 3' end. The truncated *SPL9* promoter *proSPL9trunc* was made by cloning the *SPL9* promoter and excluding a 405-bp region located -346-bp upstream of the *SPL9* start site, including the *SPL9* Regions 3 and 4 from ChIP analysis. These constructs were transformed into Col-0 and *soc1 ful* by floral dipping (Clough & Bent, 1998). The *BRI1:GUS*, *BRI1truncated-1:GUS*, *BRI1truncated-2-3:GUS*, and *BRI1truncated-1-3:GUS* lines were also constructed using the Golden Gate system (Weber *et al.*, 2011). The *BRI1* promoter (2494 bp), *BRI1* truncated-1 promoter (2277 bp), *BRI1* truncated-2-3 promoter (2022 bp), and *BRI1* truncated-1-3 promoter (1809 bp) were cloned using the primers listed in Table S2. The *BRI1* truncated-1 promoter was made by cloning the *BRI1* promoter and excluding a 217-bp region, including the *BRI1* Region 1 from ChIP analysis. The *BRI1* truncated-2-3 promoter was made by cloning the *BRI1* promoter and excluding a 472-bp region, including the *BRI1* Regions 2 and 3 from ChIP analysis. The *BRI1* truncated-1-3 promoter was made by cloning the *BRI1* promoter and excluding a 685-bp region, including the *BRI1* Regions 1, 2, and 3 from ChIP analysis. These promoter fragments were fused to the 5' end of the *GUS* cDNA, and the constructs were transformed into Col-0 and *spl* quadruple by floral dipping (Clough & Bent, 1998).

β -Glucuronidase staining analysis

β -glucuronidase staining was performed as described previously (Hu *et al.*, 2023). Whole inflorescences were prefixed in cold 90% acetone on ice for 10 min and then vacuumed for 10 min in GUS washing buffer (100 mM potassium phosphate buffer, pH 7.0, with 2 mM potassium ferricyanide, 2 mM potassium ferrocyanide, and 0.2% Triton X-100). The plant tissues were then vacuumed for 10 min in GUS staining buffer (100 mM potassium phosphate buffer, pH 7.0, with 2 mM potassium ferricyanide, 2 mM potassium ferrocyanide, 0.2% Triton X-100, and 2 mM X-Gluc) and subsequently incubated at 37°C overnight in the same GUS staining buffer. Tissues were washed with 70% ethanol three times to remove Chl.

Leaf decolorization treatment

The first cauline leaf and the last cauline leaf, at a blade length of 3–4 mm each, were harvested. Leaf tissues were incubated at room temperature in 100% ethanol, and the ethanol was replaced every 30 min until the leaf tissues became colorless. The leaves were then incubated in 75% ethanol for 5 min, followed by incubation in a solution containing 0.24 N HCl in 20% methanol at 37°C for 15 min. Subsequently, the leaves were incubated in a solution of 7% NaOH in 60% ethanol at room temperature for 15 min. The leaves were then incubated in 40, 20, 10, and 5% ethanol for 5 min each. The leaves were incubated in 25% glycerol for 15 min, stored in 50% glycerol, and analyzed on glass slides.

Imaging

Plants were imaged using a Canon EOS Rebel T7i or an Epson Perfection V600 Photo Scanner. Decolorized leaves for stomatal data were imaged using a Carl Zeiss LSM700 Confocal Microscope at 40 \times magnification. Cauline leaf blade length : width ratios were measured by the IMAGEJ software (imagej.nih.gov).

RT-quantitative PCR

RNA extraction and qPCR were performed as described previously (Hu *et al.*, 2023; Manuela & Xu, 2024). Shoot apices from each genotype were harvested in liquid nitrogen and ground into fine powder in liquid nitrogen. Total RNA was extracted using TRIzol (Thermo Fisher Scientific) and treated with Turbo DNase (Thermo Fisher Scientific) according to the manufacturer's instructions. cDNA was synthesized by reverse transcription from 1 μ g of RNA using SuperScript IV reverse transcriptase (Thermo Fisher Scientific, Waltham, MA, USA). Quantitative PCR was performed using GoTaq Hot Start (M5001; Promega) and EvaGreen dye (#31 000; Biotium, Fremont, CA, USA) using a Bio-Rad CFX96 Real-Time System. Each reverse transcription quantitative polymerase chain reaction (RT-qPCR) experiment was performed with three biological replicates, and ACTIN2 (ACT2, AT3G18780) was used as a

reference gene for quantification analysis. Primers used for RT-qPCR are listed in Table S3.

Chromatin immunoprecipitation qPCR assay

Chromatin immunoprecipitation was performed as described previously (Hu *et al.*, 2023; Manuela & Xu, 2024). Three grams of 11- or 14-d-old plants grown in LD conditions was harvested and crosslinked in 1% formaldehyde for 15 min total and vacuum-infiltrated twice for 3 min each. Tissues were then ground in liquid nitrogen and suspended in extraction buffer one (0.4 M sucrose, 10 mM Tris-HCl, pH 8.0, 10 mM MgCl₂, 5 mM β-mercaptoethanol, 1 mM phenylmethylsulfonyl fluoride (PMSF), and 0.1% TritonX-100). Pellets were washed with extraction buffer 2 (0.25 M sucrose, 10 mM Tris-HCl, pH 8.0, 10 mM MgCl₂, 5 mM β-mercaptoethanol, 1 mM PMSF, and 1% TritonX-100) and then resuspended in nuclei lysis buffer (50 mM Tris-HCl, pH 8.0, 10 mM ethylenediaminetetraacetic acid (EDTA), and 1% SDS). DNA was diluted in buffer (1.2 mM EDTA, 16.7 mM Tris-HCl, pH 8.0, 167 mM NaCl, and 0.01% SDS) and then sonicated using a Covaris ultrasonicator M220. One percent of antibodies against GFP (A11122; Invitrogen) were used in immunoprecipitation (IP). The IP protein and DNA were reverse-crosslinked to isolate the DNA using the QIA Quick PCR Purification Kit (Qiagen). The ChIP-qPCR was performed using GoTaq Hot Start (M5001; Promega), EvaGreen dye (#31 000; Biotium), and a Bio-Rad CFX96 Real-Time System. The qPCR value of ChIP samples was normalized to the value of *LFY* for SOC1-GFP ChIP, TARGET OF EAT1 (*TOE1*) for FUL-GFP ChIP, and SOC1 for rSPL9-GFP ChIP. *LEAFY* is a direct target of SOC1 and its percentage of input relative to Col-0 was set to be 1, and fold enrichment in *SPL9/15* fragments was normalized to *LFY*. *TOE1* is a direct target of FUL, and fold enrichment in *SPL9/15* fragments was normalized in the same way. *SOC1* is a direct target of SPL9, and its percentage of input relative to Col-0 was set to be 1, and fold enrichment in *BRI1* fragments was normalized to *SOC1*. Col-0 WT plants served as the negative genetic control for anti-GFP ChIP, and TA3 (AT1G37110) served as the negative control locus for ChIP-qPCR. Chromatin immunoprecipitation was performed on three sets of biological replicates each, and primers used for ChIP analysis are listed in Table S4.

Results

miR156-targeted SPL transcription factors function redundantly to promote cauline leaf identity

Previous analyses of miR156-targeted SPLs have demonstrated that they have multiple functions during vegetative and reproductive development (Xu *et al.*, 2016). In addition to promoting adult leaf identity during vegetative development, they also activate the expression of floral meristem identity genes following floral induction (Wang *et al.*, 2009; Wu *et al.*, 2009; Xu *et al.*, 2016). We have previously shown that decreased *SPL* activity in plants that overexpress miR156 or in the

spl2/9/10/11/13/15 sextuple mutant led to increased cauline leaf numbers on the primary inflorescence in LD conditions, suggesting a prolonged intermediate phase of growth and a delay in the initiation of floral meristems (Wu & Poethig, 2006; Xu *et al.*, 2016). To further reveal how individual miR156-targeted SPLs regulate cauline leaf development, we carried out a detailed analysis of cauline leaf initiation and morphology in *spl2*, *spl9*, *spl10*, *spl11*, *spl13*, *spl15*, *spl9/13*, and *spl9/15* mutants. Similar to our previous findings, *spl2*, *spl9*, *spl10*, *spl11*, *spl13*, *spl15*, *spl9/13*, and *spl9/15* mutants exhibited the same number of cauline leaves on the primary inflorescence as Col-0 (Fig. S1b). Closer morphological examination, however, revealed that while cauline leaves in Col-0 become progressively elongated (increased leaf blade length : width ratio) acropetally, cauline leaves were rounder throughout development and barely increased in blade length : width ratio in *spl9* (Figs 1d, S1c). Examination of *spl9/13* and *spl9/15* double mutants showed that cauline leaf morphology was no different to *spl9* (Figs 1d, S1c). We also examined cauline leaf number on secondary inflorescence shoots. We observed no effect of single *spl* mutants on the first and second secondary inflorescence branches but a significant increase in cauline leaf number on the third secondary inflorescence branch in *spl9* (Fig. S1e). This effect was enhanced and extended to the first and second secondary inflorescence shoots in *spl9/15* but not in *spl9/13* (Fig. S1e). Together, these results suggest that changes to cauline leaf morphology can occur independently of floral meristem initiation and that *SPL9* has a unique role in cauline leaf development.

To confirm that the limited phenotypic effects of *spl* single mutants are not due to a lack of expression in cauline leaves, we examined the staining patterns of miR156-sensitive GUS translational fusions for *SPL2*, *SPL9*, *SPL10*, *SPL11*, *SPL13*, and *SPL15* that we previously generated (Xu *et al.*, 2016). All of the *SPL::SPL-GUS* fusions were expressed in the cauline leaves, stems, and flowers of young inflorescences, with *SPL9* and *SPL13* expressed the strongest in cauline leaves (Fig. 1a). Next, we examined the primary inflorescences in higher order *spl* mutants, which revealed that the *spl9/13/15* triple mutant and the *spl2/9/13/15* quadruple mutant (*spl qm*) have one more cauline leaf than Col-0, while the *spl2/9/10/13/15* quintuple mutant and the *spl2/9/10/11/13/15* sextuple mutant (*spl sxm*) have two to three more cauline leaves than Col-0 (Fig. 1b). We then quantified cauline leaf morphology and counted the number of leaves on each secondary inflorescence. Our results showed that the cauline leaves from the *spl9/13*, *spl9/15*, *spl9/13/15*, *spl2/9/13/15*, *spl2/9/10/13/15*, and the *spl2/9/10/11/13/15* mutants were all rounder (smaller blade length : width ratio) than in Col-0, that all mutant combinations exhibited limited heteroblastic developmental changes, and that there was no additional effect of *spl2/10/11* on leaf blade development in the *spl9/13/15* background (Fig. 1c,d). However, there is greater genetic redundancy in the repression of petiole development. Petioles on cauline leaves start to emerge in the *spl9/13/15* triple mutant and increase in length as *SPL* activity decreases, with the *spl sxm* exhibiting the longest and most clearly distinguished petioles (Fig. 1c). Correspondingly, the number of leaves on each of the secondary

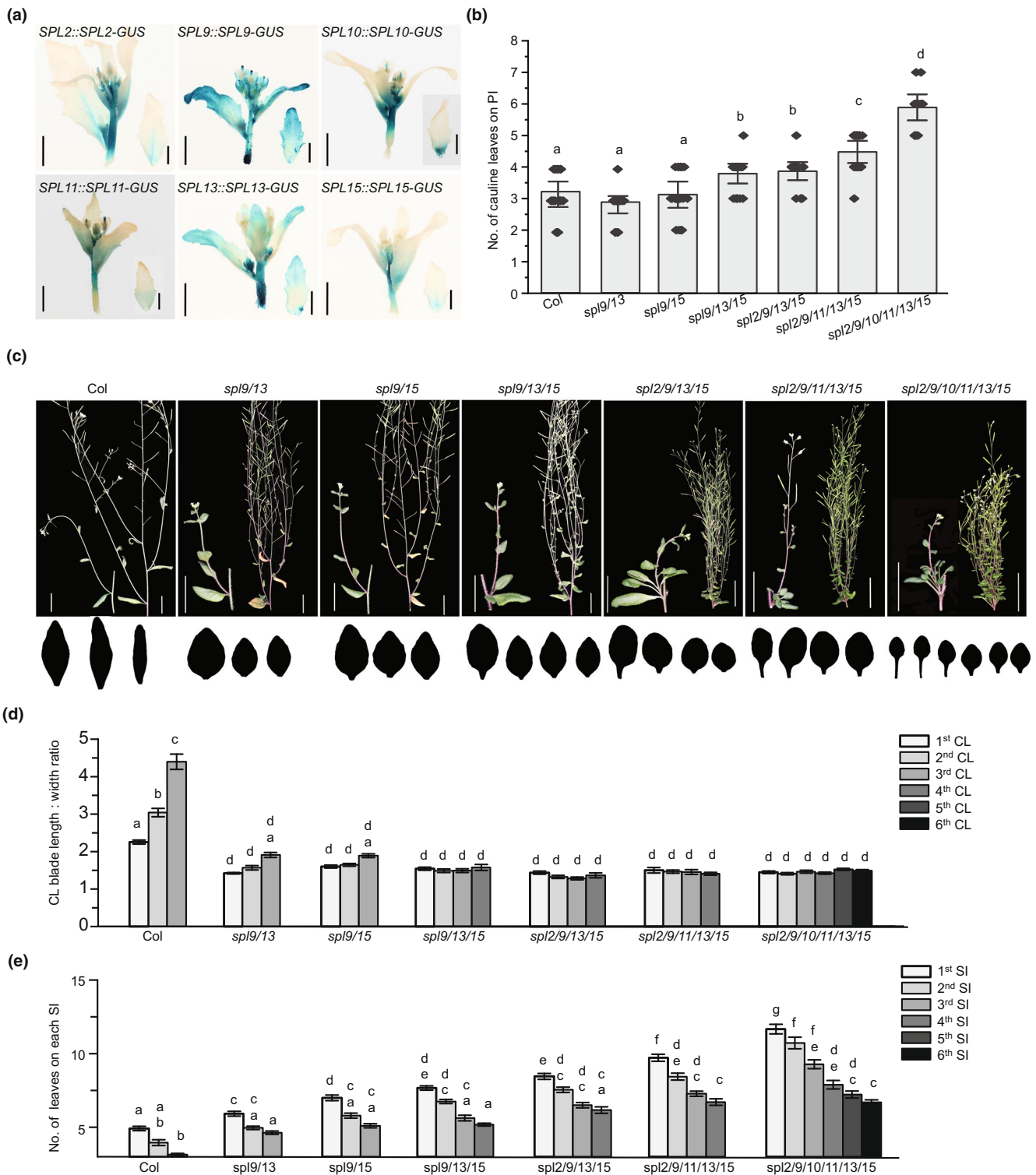


Fig. 1 miR156-targeted SQUAMOSA PROMOTER BINDING PROTEIN-LIKE (SPL) transcription factors function redundantly to promote cauline leaf identity in *Arabidopsis*. (a) Expression of *SPL2*, *SPL9*, *SPL10*, *SPL11*, *SPL13*, and *SPL15* in cauline leaves (CL). Bars, 3 mm. Five to six biological replicates were examined for each genotype. (b) Number of cauline leaves on primary inflorescence (PI) in *spl* mutants. One-way ANOVA, $P < 0.05$, different letters above each graph represent significantly different groups. (c–e) Loss-of-function in *spl* mutants changes the overall look of the inflorescences (c), cauline leaf shape (d), and the number of leaves on each secondary inflorescence (SI) that each cauline leaf is associated with (e). Bars, 2 cm. (d, e) Two-way ANOVA, $P < 0.05$, different letters above each graph represent significantly different groups. Error bars represent SE.

inflorescences increased significantly in progressively higher order mutants. For the first secondary inflorescence, Col-0 has *c.* 5 leaves, *spl9/15* have *c.* 7 leaves, *spl9/13/15* have *c.* 7.5 leaves, *spl2/9/13/15* have *c.* 8.5 leaves, *spl2/9/10/13/15* have *c.* 10 leaves, and the *spl sxm* have *c.* 12 leaves (Fig. 1e). Therefore, these results suggest that miR156-targeted SPLs function redundantly in determining both cauline leaf morphology and the number of cauline leaves on primary and secondary inflorescence shoots.

Mutations in the master regulator of floral meristem identity *LFY* also result in higher rates of cauline leaf initiation on primary and secondary inflorescence shoots due to defective floral meristem specification (Weigel *et al.*, 1992). To determine whether SPLs function similarly to *LFY*, we examined the cauline leaf number, cauline leaf shape, and the number of leaves on each secondary inflorescence of the strong loss-of-function mutant *lfy-1* (Weigel *et al.*, 1992). Our results showed that *lfy-1* made approximately nine more cauline leaves than Col-0, much more than the *spl sxm* (Fig. S3a,b). However, overall cauline leaf shape was similar in *lfy-1* and Col-0, with blade length : width ratio also increasing acropetally in *lfy-1* (Fig. S3c,d). As on the primary inflorescence, the number of leaves on each *lfy-1* secondary inflorescence is also much more than that of Col-0 (Fig. S3e). Together, these results suggest that *SPL* genes and *LFY* function differently in the regulation of inflorescence shoot architecture. Loss of *LFY* function results in more cauline leaves on both the primary and secondary inflorescences, presumably due to perturbed floral meristem initiation. However, there is little effect on cauline leaf morphology in *lfy-1*. On the other hand, miR156-targeted *SPL* genes have specific functions in promoting cauline leaf identity, as loss-of-function mutants produce drastically different cauline leaves. *SPL2/9/10/11/13/15* also have a minor role in promoting floral meristem identity, as *spl2/9/10/11/13/15* mutants produce more cauline leaves than Col-0 (Xu *et al.*, 2016).

Floral activators promote *SPL* gene expression during floral induction

Cauline leaves initiate at the end of vegetative development when levels of miR156 are persistently low (Xu *et al.*, 2016), suggesting that any effects of *SPL2/9/10/11/13/15* on cauline leaf identity are likely to be miR156-independent. It has previously been shown that *SPL* genes are significantly upregulated during floral induction, indicating that they may be activated by floral induction pathways (Schmid *et al.*, 2003). To test this, we first examined the transcript levels of *SOC1*, *FUL*, *FD*, *CO*, *AGL24*, and *AGL42*, activators for *LFY* and *API* (Samach *et al.*, 2000; Wigge *et al.*, 2005; Liu *et al.*, 2008; Torti & Fornara, 2012; Balanzà *et al.*, 2014), and miR156-targeted *SPL2*, *SPL9*, *SPL10*, *SPL11*, *SPL13*, and *SPL15*, in a *35S:MIM156* line in which miR156 has been sequestered (Wu *et al.*, 2009). Therefore, any changes in transcript levels will be miR156-independent. *35S:MIM156* plants were first grown in SD conditions for 2 wk and then transferred to LD conditions to induce flowering. Shoot apices before the transfer to LD conditions (D0) and after 3 d in LD conditions (D3) were harvested for RT-qPCR analysis. The expression

of each of the floral activators increased following transfer to LD conditions in *35S:MIM156* plants (Fig. 2a). Correspondingly, expression levels of *SPL2*, *SPL9*, *SPL10*, *SPL11*, *SPL13*, and *SPL15* also increased upon floral induction at D3 in *35S:MIM* plants, but at lower levels than the floral activators (Fig. 2a). These results are consistent with a model in which *SPL* genes are promoted by *SOC1*, *FUL*, *FD*, *CO*, *AGL24*, and/or *AGL42* during floral induction.

To examine whether these floral activators regulate *SPL2/9/10/11/13/15* expression during floral induction, we examined *SPL* transcript levels in plants overexpressing *SOC1*, *FUL*, *FD*, *CO*, *AGL24*, and *AGL42*. Consistent with previous results (Samach *et al.*, 2000; Wigge *et al.*, 2005; Liu *et al.*, 2008; Balanzà *et al.*, 2014), the expression of the flowering activators driven by the constitutive *35S* promoter induced early flowering (Figs 2b, S4a). Consistent with the hypothesis that floral activators promote *SPL* expression, we found that *35S:SOC1*, *35S:FUL*, *35S:CO*, *35S:AGL24*, and *35S:AGL42* produced fewer juvenile leaves than Col-0 (Figs 2b, S4b). Reverse transcription quantitative polymerase chain reaction analyses of *SPL* transcript levels were carried out at 11 d after the germination of plants grown in LD conditions when levels of miR156 were not significantly different between the transgenic plants and Col-0 (Fig. 2c). The relative expression of *SPL2*, *SPL9*, *SPL10*, *SPL11*, and *SPL15* was significantly higher in *35S:SOC1*, *35S:FUL*, *35S:CO*, and *35S:AGL24* (Fig. 2d–i), with the strongest induction consistently observed in *35S:SOC1* and *35S:FUL* (Fig. 2d–i) than Col-0. *SPL13* transcript levels were significantly higher in *35S:FUL*, *35S:CO*, and *35S:AGL24*, although overall expression remained lower than that of other *SPL* genes examined. We observed no effects on *SPL* transcript levels in *35S:FD*, consistent with the lack of an effect on vegetative phase change in this line (Fig. 2b). Only *SPL9* and *SPL15* were upregulated in *35S:AGL42* (Fig. 2c–i). These results indicate that multiple floral activators, particularly *SOC1*, *FUL*, *CO*, and *AGL24*, induce *SPL* gene expression and that they regulate *SPL* activity independent of miR156.

Ectopic expression of miR156 driven by promoters of floral activators resulted in a delay of cauline leaf identity

We hypothesized that if floral activators endogenously upregulate *SPL* gene expression in cauline leaves, then they should be expressed in cauline leaves. Therefore, we analyzed the expression of *SOC1*, *FUL*, *FD*, *CO*, *AGL24*, and *AGL42* in the cauline leaves of young inflorescences using *PROMOTER:GUS* reporter fusions. Our results showed that the promoters of *SOC1*, *FUL*, and *CO* are active throughout cauline leaves, while *FD*, *AGL24*, and *AGL42* promoter expression is limited to the basal part of cauline leaves (Fig. 3a).

Next, we reasoned that if floral activators induce *SPL* activity in cauline leaves transcriptionally, then the ectopic expression of miR156 driven by floral activator promoters would phenocopy the cauline leaf phenotype of *spl* mutants. To test this, we quantified cauline leaf morphology and number in Col-0 and transgenic plants expressing *SOC1:MIR156A*, *FUL:MIR156A*, *FD:MIR156A*, *CO:MIR156A*, *AGL24:MIR156A*, and *AGL42:*

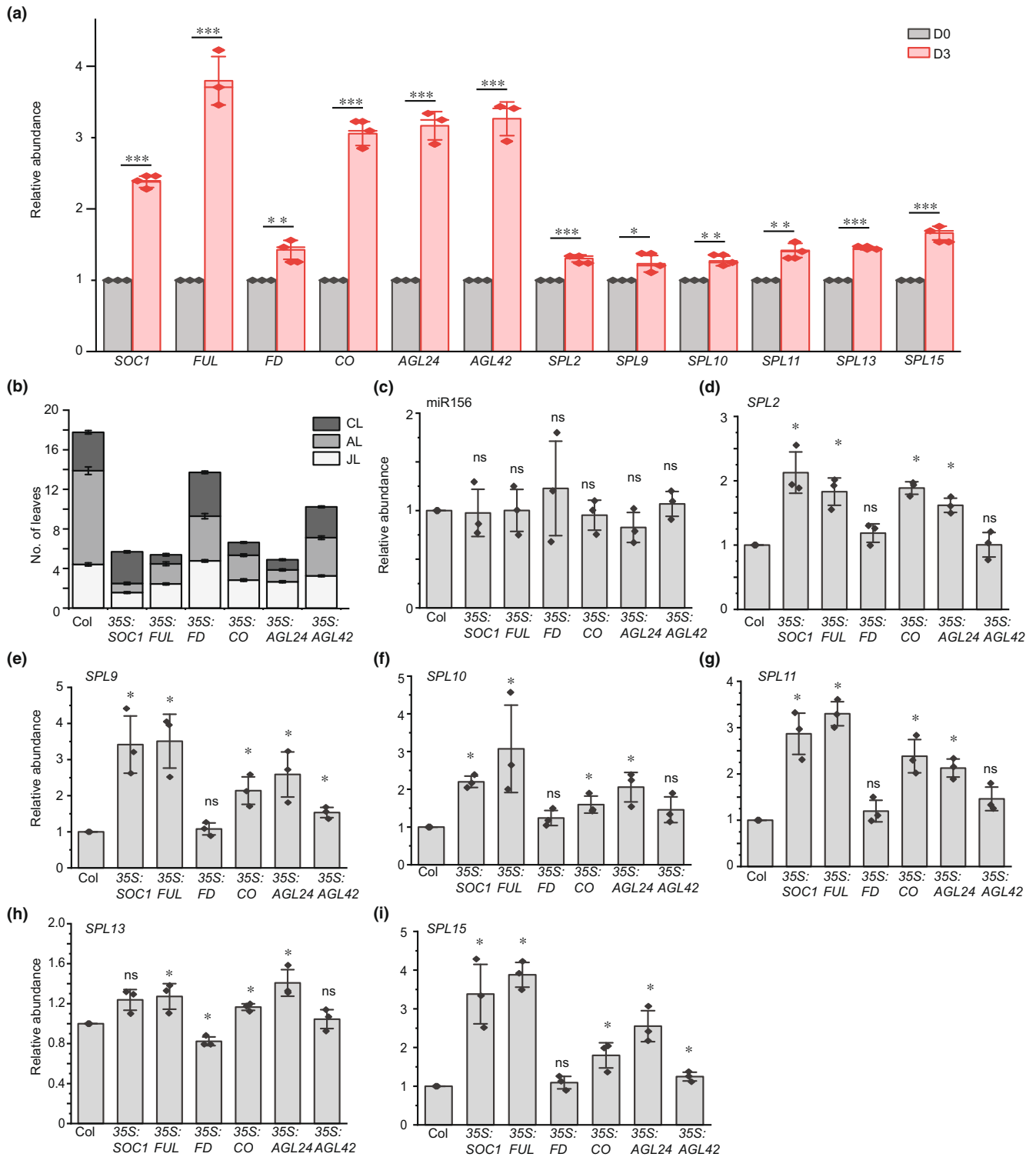


Fig. 2 Floral induction promotes the expression of miR156-targeted SQUAMOSA PROMOTER BINDING PROTEIN-LIKE (SPL) genes in *Arabidopsis*. (a) Expression of floral activators and *SPL2*, *SPL9*, *SPL10*, *SPL11*, *SPL13*, *SPL15* in 35S:*MIM156* before and after floral induction in cauline leaves. Plants were grown in short-day (SD) conditions for 2 wk (D0) and transferred to long-day (LD) conditions for 3 d (D3). (b) The number of juvenile leaves (JL), adult leaves (AL), and cauline leaves (CL) in Columbia (Col-0) and plants overexpressing SUPPRESSOR OF OVEREXPRESSION OF CONSTANS1 (*SOC1*), FRUITFUL (*FUL*), *FD*, CONSTANS (*CO*), AGAMOUS-like24 (*AGL24*), and *AGL42*. (c–i) Relative levels of *miR156* (c), *SPL2* (d), *SPL9* (e), *SPL10* (f), *SPL11* (g), *SPL13* (h), and *SPL15* (i) in 11-d-old Col-0 and plants overexpressing *SOC1*, *FUL*, *FD*, *CO*, *AGL24*, and *AGL42*. *, $P < 0.05$; **, $P < 0.01$; ***, $P < 0.001$; ns, not significantly different, $P > 0.05$, *t*-test or one-way ANOVA. Error bars represent SE.

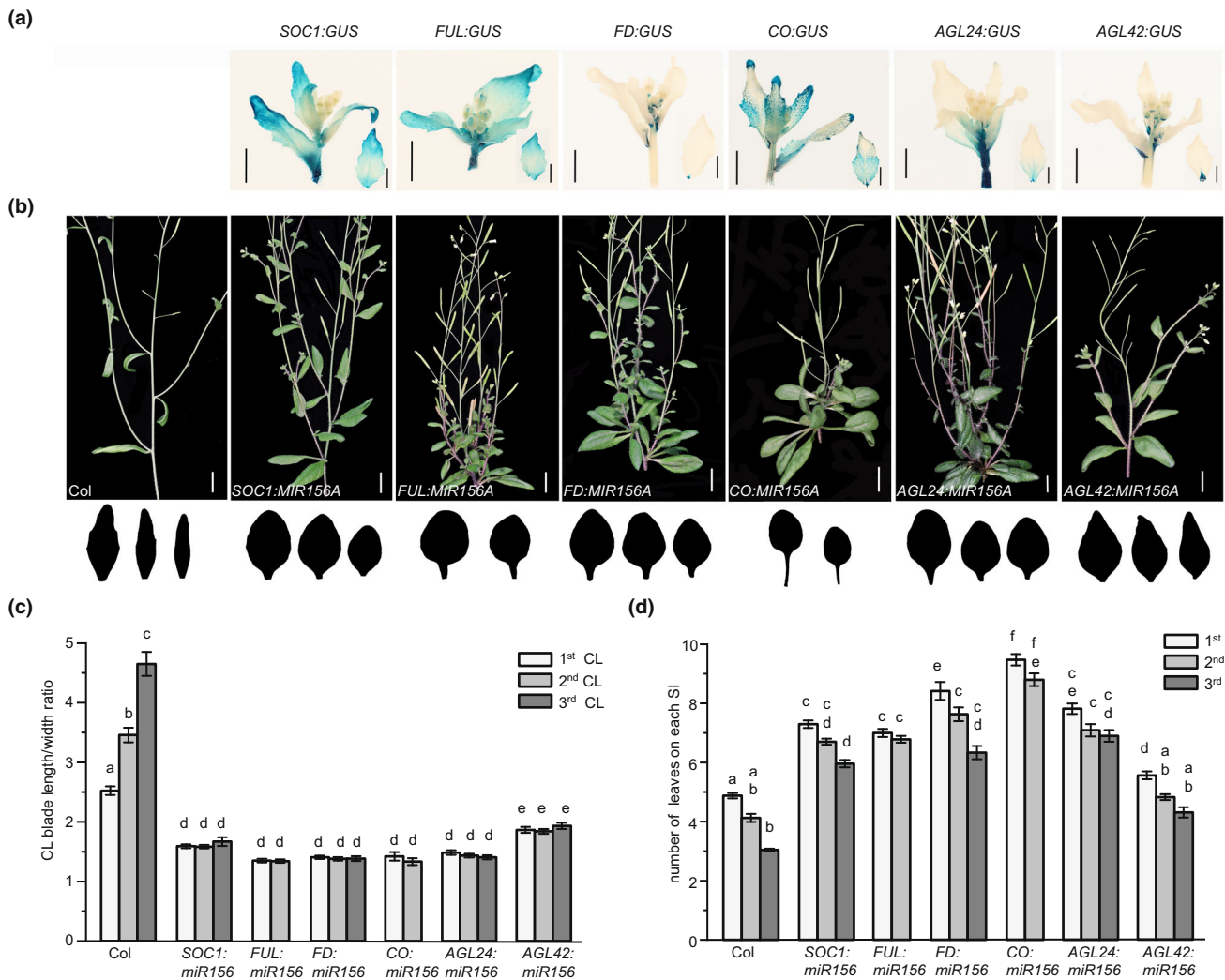


Fig. 3 Ectopic expression of miR156 in cauline leaves driven by floral activators resulted in rounder cauline leaves and more leaves produced on each of the secondary inflorescences in *Arabidopsis*. (a) Expression of SUPPRESSOR OF OVEREXPRESSION OF CONSTANS1 (*SOC1*), FRUITFUL (*FUL*), *FD*, CONSTANS (*CO*), AGAMOUS-like24 (*AGL24*), and *AGL42* in cauline leaves. Bars, 3 mm. (b) Inflorescences and cauline leaves from plants ectopically expressing *MIR156A* driven by *SOC1*, *FUL*, *FD*, *CO*, *AGL24*, and *AGL42*. Bars, 1 cm. (c, d) Cauline leaf length : width ratio (c) and the number of leaves on each secondary inflorescence (d) in plants ectopically expressing *MIR156A* driven by *SOC1*, *FUL*, *FD*, *CO*, *AGL24*, and *AGL42*. Shared letters above each group indicate not significantly different groups; different letters above each group indicate significantly different groups. $P < 0.05$, two-way ANOVA. Error bars represent SE.

MIR156A (Fig. 3b–d). We observed no increase in the number of cauline leaves on the primary inflorescence in any of the transgenic lines (Fig. S5); however, all lines produced significantly rounder cauline leaves with no acropetal heteroblastic change in leaf shape (Fig. 3b,c). Furthermore, distinct petioles emerged in the cauline leaves of the transgenic lines (Fig. 3b). These were most apparent in *CO:MIR156A* but were also visible in *SOC1:MIR156A*, *FUL:MIR156A*, *FD:MIR156A*, and *AGL24:MIR156A* lines (Fig. 3b). Each of these transgenic lines also produced significantly more leaves on their secondary inflorescences than Col-0 (Fig. 3d). However, the effects of *AGL42:MIR156A* on petiole production and cauline leaf number were limited. The phenotypes of plants expressing *MIR156A* from floral activator promoters were similar to loss-of-function *spl* mutants (Fig. 1c). Taken together, these results are consistent with the hypothesis

that *SPLs* function downstream of floral activators in promoting cauline leaf development.

SOC1 and FUL are the major floral inducers that promote cauline leaf identity

To further characterize the roles of floral activator genes during cauline leaf development, we analyzed a series of loss-of-function mutants: *agl24-3* (hereafter *agl24*), *agl42-crispr* (CRISPR-Cas9 induced mutation – this study, hereafter *agl42*), *fd-3* (hereafter *fd*), *co-10* (hereafter *co*), *soc1-2* (hereafter *soc1*), *ful-2* (hereafter *ful*), *agl24 ful*, *agl42 ful*, *agl24 agl42*, *soc1 ful*, *soc1 agl24*, and *soc1 agl42* (Fig. 4). During rosette development, each of these mutants produced the same number of juvenile leaves; however, they produced more adult leaves than Col-0 as a result of their delayed flowering

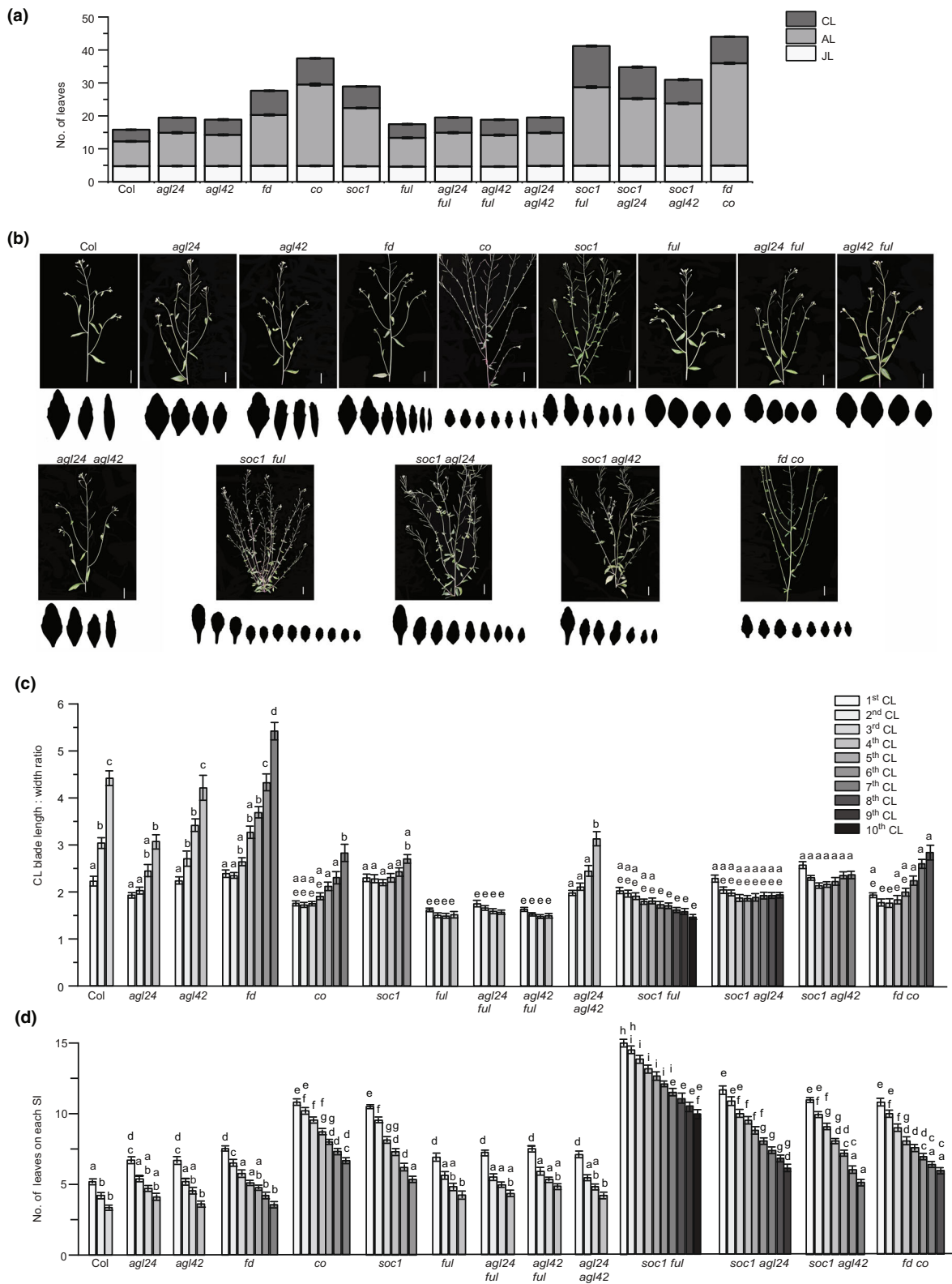


Fig. 4 Mutations in SUPPRESSOR OF OVEREXPRESSION OF CONSTANS1 (*SOC1*), FRUITFUL (*FUL*), *FD*, CONSTANS (*CO*), AGAMOUS-like24 (*AGL24*), and *AGL42* result in rounder cauline leaves and more leaves on each secondary inflorescence in *Arabidopsis*. (a) Number of juvenile leaves, adult leaves, and cauline leaves in loss-of-function floral activator single and double mutants. (b) Shoot architecture and indication of heteroblasty in cauline leaves on the primary inflorescence. Bars, 2 cm. (c, d) Statistical analysis on cauline leaf shape (length : width ratio) on the primary inflorescence (c) and the number of leaves on each secondary inflorescence (d). Shared letters above each bar indicate not significantly different groups; different letters above each bar indicate significantly different groups, $P < 0.05$, two-way ANOVA. Error bars represent SE.

(Fig. 4a). Among the single mutants, all *ful* cauline leaves were rounder than in Col-0, while *soc1* and *co* single mutants produced rounder leaves than Col-0 from the second cauline leaf onward (Fig. 4b,c). All the double-mutant combinations we tested exhibited rounder cauline leaves throughout development except for *agl24 agl42*, in which the first cauline leaf appeared WT, but subsequent leaves were significantly rounder (Fig. 4b,c). Furthermore, the cauline leaves of *soc1 ful*, *soc1 agl24*, and *soc1 agl42* produced petioles (Fig. 4b). All of the flowering-time mutants produced more cauline leaves on primary and secondary inflorescence shoots (Fig. 4b–d). Of these mutants, *soc1 ful* had the severest cauline leaf phenotype, exhibiting the roundest leaves, most elongated petioles, and the largest number of cauline leaves on primary and secondary inflorescences (Fig. 4b–d). The phenotypic similarities of the cauline leaves in *soc1 ful* and higher order *spl* mutants further support the idea that *SOC1*, *FUL*, and *SPL* genes may function in a common pathway to promote cauline leaf identity.

To test whether *SOC1* and *FUL* mask the activity of other floral activators, we generated a series of higher order mutants in a *soc1 ful* background: *soc1 ful agl24*, *soc1 ful agl42*, *soc1 ful agl24 agl42*, *soc1 ful agl24 agl42 fd*, *soc1 ful agl24 agl42 co*, and *soc1 ful agl24 agl42 fd co*. Each of these mutants produced the same number of juvenile leaves as *soc1 ful* but more adult leaves, increasing as additional mutant alleles were introduced (Fig. 5a). The number of cauline leaves, cauline leaf blade length : width ratios, and the number of leaves on each secondary inflorescence, however, remained similar to *soc1 ful* (Fig. 5b–e). This confirms that *SOC1* and *FUL* are key players among floral activators in promoting cauline leaf identity and suggests that *AGL24*, *AGL42*, *FD*, and *CO* likely function in the same pathway as *SOC1* and *FUL* in promoting cauline leaf identity.

SOC1 and FUL directly promote SPL gene expression

To determine whether the *soc1 ful* cauline leaf phenotypes are associated with changes in the expression of *SPL* genes, we performed RT-qPCR analyses on Col-0, *soc1*, *ful*, and *soc1 ful* shoot apices at Day 18, when miR156 levels were similarly low across all genotypes (Fig. 6a). We found that *SPL2*, *SPL9*, *SPL10*, *SPL11*, and *SPL15* transcript levels were significantly lower in *soc1*, *ful*, and *soc1 ful* mutants, whereas levels of *SPL13* were unaffected (Fig. 6a). To test for genetic redundancy at the molecular level, we also quantified transcript levels in higher order floral activator mutants in a *soc1 ful* background. We saw no difference in the levels of *SPL2*, *SPL9*, *SPL10*, *SPL11*, and *SPL15* transcripts in *soc1 ful agl24*, *soc1 ful agl24 agl42*, *soc1 ful agl24 agl42 co*, and *soc1 ful agl24 agl42 co fd* plants relative to *soc1 ful* (Fig. 6b). Taken together, the results of our phenotyping and RT-qPCR analyses support a regulatory interaction between the floral induction and the miR156/*SPL* pathways in the specification of cauline leaf identity and suggest that *SOC1* and *FUL* have larger effects on cauline leaf development than other floral activator genes. However, as the tissue we used for our gene expression analyses included floral and shoot tissue as well as initiating cauline leaves, we cannot spatially resolve where the genetic interaction between the floral activators and *SPL* genes occurs.

Of the *SPL* genes we tested, the expression of *SPL9* and *SPL15* was most strongly upregulated in *35S::SOC1* and *35S::FUL* plants (Fig. 2e,i) and most strongly suppressed in *soc1 ful* (Fig. 6a,b). To investigate whether *SOC1* and *FUL* directly activate *SPL9* and *SPL15* to promote cauline leaf identity, we performed ChIP-qPCR using a novel *SOC1::SOC1-GFP soc1* line (Fig. S6) and a previously reported *35S::FUL-GFP* line (Manuela & Xu, 2024). We grew these plants in LD conditions and harvested tissue from *SOC1::SOC1-GFP soc1* at Day 14 and *35S::FUL-GFP* at Day 11. The candidate binding sites for *SOC1* and *FUL* upstream of the *SPL9* and *SPL15* start codons were identified using prior genome-wide analyses of MADS-box transcription factor binding sites (Tao *et al.*, 2012; van Mourik *et al.*, 2023). Primers specific to the candidate binding sites were designed to test for target enrichment in chromatin immunoprecipitated with antibodies to GFP (Fig. 6c,d). Consistent with previous reports (Lee *et al.*, 2008; Liu *et al.*, 2008; Balanzà *et al.*, 2018), we found that *SOC1* and *FUL* bind to *LFY* and *TOE1*, respectively. We therefore normalized our ChIP-qPCR data to the binding of *SOC1* to *LFY* and of *FUL* to *TOE1* (Fig. 6e,f). The locus of the retrotransposon *TA3* was used as a negative control. Our results show that *SOC1* and *FUL* directly bind to the same sites in the *SPL9* promoter (*SPL9-3*, *SPL9-4*), between 340 and 747-bp upstream of the start codon (Fig. 6c–f). Both *SOC1* and *FUL* also bind directly to the same site on the *SPL15* promoter (*SPL15-2*), and *SOC1* binds to an additional site on the *SPL15* promoter that *FUL* does not (*SPL15-3*), between 290-bp and 700-bp upstream of the start codon (Fig. 6c–f). Our data indicate that *SOC1* and *FUL* converge on the same regulatory regions of *SPL9* and *SPL15* to promote gene expression.

To verify our ChIP data, we generated a truncated *SPL9* promoter-GUS fusion construct lacking the *SOC1* and *FUL* binding sites *SPL9-3* and *SPL9-4* (Fig. 6c). We reasoned that if these sequences are required to activate *SPL9* expression during cauline leaf development, then a GUS reporter construct missing them (*SPL9truncated::SPL9-GUS*) will be less strongly expressed in cauline leaves than a GUS reporter construct driven by the intact *SPL* promoter sequence (*SPL9::SPL9-GUS*). *SPL9::SPL9-GUS* expression was strongly detected in the cauline leaves, stems, and flowers of young inflorescences (Fig. 6g), consistent with a previous analysis (Xu *et al.*, 2016). By contrast, *SPL9truncated::SPL9-GUS* showed strong expression in stems and flowers but only weak expression in the veins of cauline leaves (Fig. 6g), suggesting that specific regulatory sequences in the *SPL9* promoter are required for expression in cauline leaves. Furthermore, in a *soc1 ful* mutant background, *SPL9::SPL9-GUS* expression persisted in the stem and young flowers but was absent in cauline leaves (Fig. 6g), confirming a spatially restricted interaction between redundant MADS-box transcription factors and *SPL9*.

SPL genes are necessary for SOC1 and FUL function during cauline leaf development

Our results thus far indicate that several miR156-targeted *SPLs* function directly downstream of *SOC1* and *FUL* to promote cauline leaf identity. If this is the case, then increased *SOC1* or *FUL*

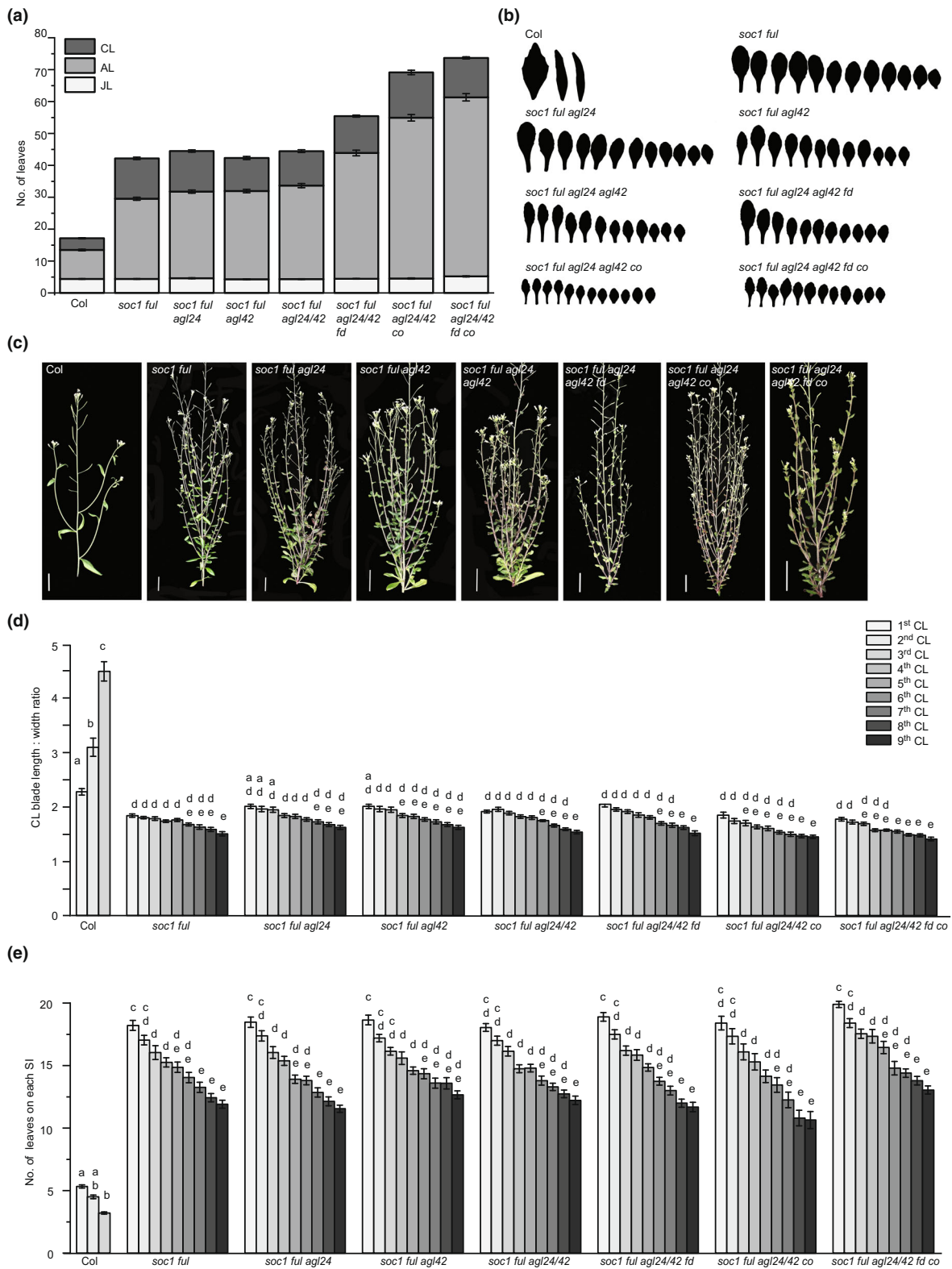


Fig. 5 Loss of additional floral regulator function in a *soc1 ful* background does not affect cauline leaf identity in *Arabidopsis*. (a) Number of juvenile leaves, adult leaves, and cauline leaves in loss-of-function floral activator double, triple, quadruple, quintuple, and sextuple mutants. (b) Cauline leaf heteroblasty in Columbia (Col-0), *soc1 ful*, and higher order *soc1 ful* mutants. (c) Plant shoot architecture. Bars, 2 cm. (d, e) Statistical analysis on cauline leaf shape (length : width ratio) (d) and number of leaves on each secondary inflorescence (e) in Col-0, *soc1 ful*, and higher order *soc1 ful* mutants. Shared letters above each bar indicate not significantly different groups; different letters above each bar indicate significantly different groups, $P < 0.05$, two-way ANOVA. Error bars represent SE. FUL, FRUITFUL; SOC1, SUPPRESSOR OF OVEREXPRESSION OF CONSTANS1.

expression should have minimal effect on cauline leaf development in a *spl* mutant background. To test this hypothesis, we introduced the *35S::SOC1* and *35S::FUL* constructs into a

spl2/9/13/15 quadruple mutant background (*spl qm*). The *spl qm* produces more juvenile leaves, total rosette leaves, and cauline leaves than Col-0, whereas juvenile, rosette, and cauline leaves are

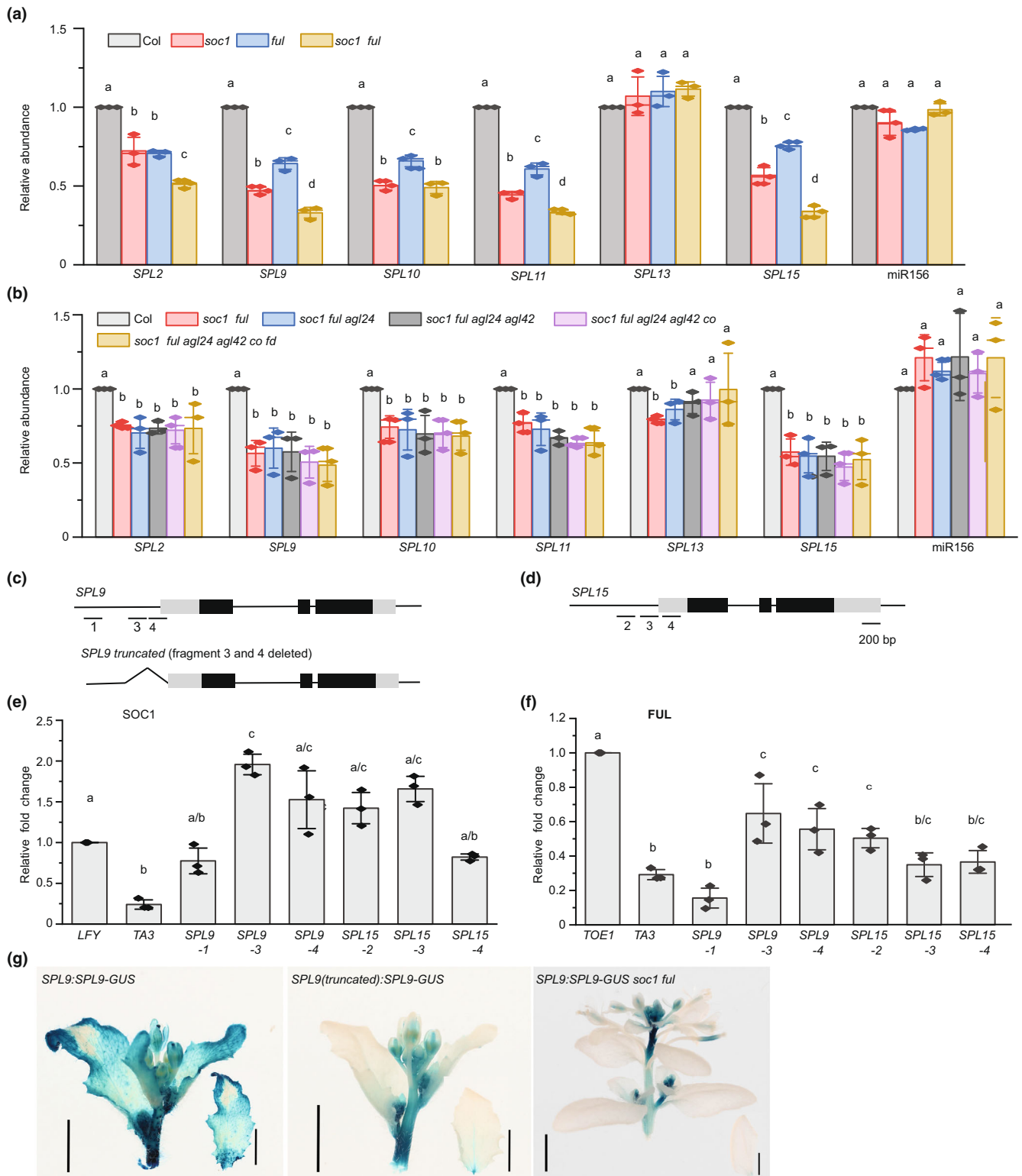


Fig. 6 SUPPRESSOR OF OVEREXPRESSION OF CONSTANS1 (SOC1) and FRUITFUL (FUL) directly promote SQUAMOSA PROMOTER BINDING PROTEIN-LIKE (SPL) gene expression in *Arabidopsis*. (a, b) Reverse transcription quantitative polymerase chain reaction (RT-qPCR) analysis of SPLs in *soc1* and *ful* mutants (a), and higher order mutants containing *soc1 ful* (b). Error bars represent SE (a, b). (c, d) Schematic diagram of SPL9 with indication of regions removed (c) and SPL15 (d) genomic DNA, with indicated positions bound by SOC1 or FUL tested in chromatin immunoprecipitation followed by qPCR (ChIP-qPCR). Gray boxes indicate untranslated region (UTR), and black boxes indicate exons. (e, f) ChIP-qPCR analysis of SOC1 and FUL binding sites of SPL9 and SPL15. LEAFY (LFY) is a direct target of SOC1, its percentage of input relative to Columbia (Col-0) was set to be 1, and fold enrichment in SPL9/15 fragments was normalized to LFY. TOE1 is a direct target of FUL, and fold enrichment in SPL9/15 fragments was normalized in the same way. The TA3 retrotransposon (AT1G37110) served as a negative control locus for ChIP-qPCR. Shared letters above each bar indicate not significantly different groups; different letters above each bar indicate significantly different groups, $P < 0.05$, two-way ANOVA (a, b), one-way ANOVA (e, f). (g) Translational β -glucuronidase (GUS) fusions of SPL9 driven by its native promoter (left), a truncated promoter (middle), or the native promoter in the *soc1 ful agl24* background (right). Bars, 3 cm. Error bars represent SE.

all reduced in *35S:SOC1* and *35S:FUL* plants (Fig. 7a–c). However, the effects of *35S:SOC1* and *35S:FUL* were entirely suppressed in the *spl qm* background. The effects of *35S:SOC1* and *35S:FUL* on shoot architecture (Fig. 7d) and cauline leaf shape (Fig. 7e,f) were also suppressed in the *spl qm*. This suggests that SPL2/9/13/15 are completely epistatic to SOC1 and FUL during cauline leaf development. However, we did observe a slight reduction in the number of cauline leaves on the first secondary inflorescence shoot when SOC1 or FUL1 was constitutively expressed in *spl qm* (Fig. 7g). This may be due to the residual activity of SPL10/11 (Shikata *et al.*, 2009; Fig. 1e) or elevated LFY activity caused by SOC1 and FUL overexpression (Lee *et al.*, 2008; Liu *et al.*, 2008; Balanzà *et al.*, 2018).

SPL genes promote stomatal differentiation in cauline leaves

Previous research has shown that miR156-targeted SPL genes regulate stomatal percentage and photosynthetic rate during vegetative development (Feng *et al.*, 2016; Lawrence *et al.*, 2021; Li *et al.*, 2024). To determine whether the miR156/SPL network regulates stomatal differentiation during cauline leaf identity, we analyzed stomata on the abaxial surface of the first and last cauline leaves in Col-0 and *spl sxm* plants at a blade length of 3–4 mm (Fig. 8a). We calculated the stomatal percentage (number of stomata/total number of epidermal cells) and examined both the tip and middle of these cauline leaves to account for differences in rates of stomatal differentiation (Le Gloanec *et al.*, 2024). Our data showed that both the first and last cauline leaves of *spl sxm* had a significantly lower stomatal percentage in the tip and middle than WT plants (Fig. 8a–c). These results suggest that SPL genes may regulate multiple aspects of cauline leaf development.

SPL9 binds to BRI1 directly to regulate cauline leaf development

Interestingly, it has previously been reported that loss-of-function of the receptor for the phytohormone BR BRI1 leads to rounder cauline leaves (Xiong *et al.*, 2021). Furthermore, the BR signaling pathway components BRASSINOSTEROID INSENSITIVE2 (BIN2) and BRASSINAZOLE-RESISTANT 1 (BZR1) were reported to genetically and physically interact with SPL9 to regulate vegetative phase change (Wang *et al.*, 2021; Zhou

et al., 2023). Therefore, we decided to test whether the SPL and BR pathways also coordinate cauline leaf identity.

As strong *bri1* alleles inhibit stem elongation, making it difficult to distinguish cauline leaves, we analyzed the weak Col-0 allele *bri1-301*. Cauline leaf shape analysis showed that the 3rd cauline leaf in *bri1-301* was significantly rounder than Col-0 (Fig. 9a,b). However, we observed no effect on cauline leaf number (Fig. S7a,b). To test whether SPLs and BRI1 interact at the transcriptional level to regulate cauline leaf identity, we performed RT-qPCR analysis of BRI1 gene expression in Col-0 and *spl sxm* mutant plants. Our results showed significantly lower BRI1 transcript levels in *spl sxm* (Fig. 9c), suggesting that SPL transcription factors promote BRI1 expression.

Next, we conducted ChIP-qPCR to determine whether SPL9 directly activates BRI1 expression using a SPL9:GFP-rSPL9 *spl9/13* transgenic line we previously generated (Hu *et al.*, 2023). ChIP-qPCR results revealed SPL9 binds to multiple regions of the BRI1 promoter and coding sequence, with particularly strong binding to sequences in the promoter (Fig. 9d,e). To further explore the functional relevance of these candidate regulatory elements, we created constructs of full-length and truncated BRI1 promoters missing specific SPL9 binding sites (Positions 1, 2, and 3) fused with GUS (Fig. 9f). The full-length BRI1 promoter (2494 bp) drove the expression of GUS broadly in cauline leaves (Fig. 9g). Analysis of the deletion constructs BRI1:GUS-1 (without Position 1), BRI1:GUS-2 (without Positions 2 and 3), and BRI1:GUS-3 (without Positions 1 to 3) showed that BRI1:GUS-1 and BRI1:GUS-3 had minimal GUS activity in cauline leaves, whereas BRI1:GUS-2 maintained activity similar to the full-length promoter (Fig. 9g). These results indicate that the sequence at Position 1 is necessary for BRI1 expression in cauline leaves, whereas the sequences at Positions 2 and 3 are not. In the *spl qm* background, plants transformed with full-length BRI1:GUS exhibited reduced GUS activity in the distal region of cauline leaves (Fig. 9g). Collectively, these findings suggest that SPL9 directly promotes BRI1 expression to regulate cauline leaf identity.

Discussion

SPLs are master regulators for cauline leaf identity

Cauline leaves exhibit specific developmental features that distinguish them from vegetative (i.e. rosette) leaves. They are

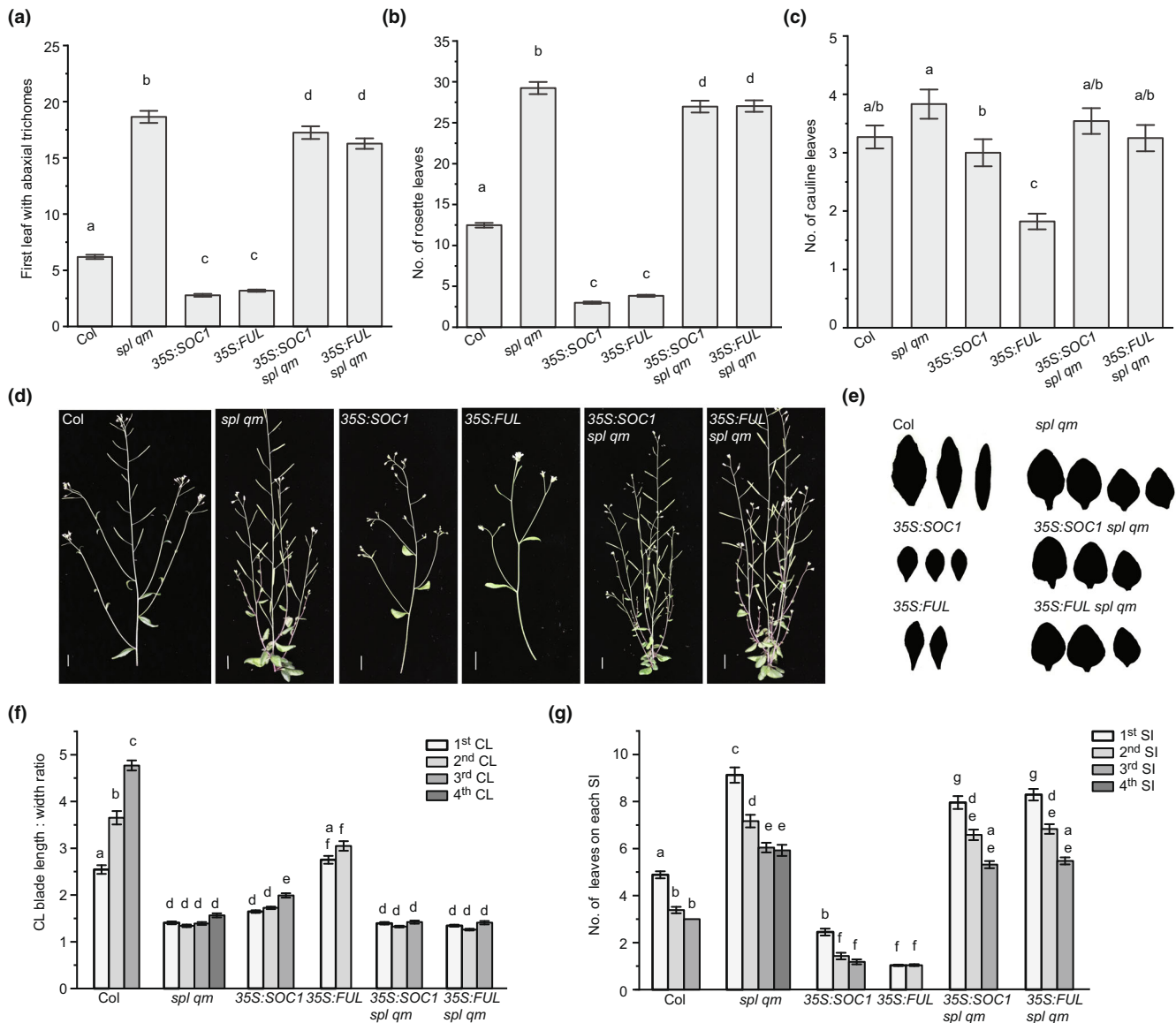


Fig. 7 SQUAMOSA PROMOTER BINDING PROTEIN-LIKE (*SPL*) genes are necessary for SUPPRESSOR OF OVEREXPRESSION OF CONSTANS1 (*SOC1*) and FRUITFUL (*FUL*) function during cauline leaf development in *Arabidopsis*. (a–g) First rosette leaf with abaxial trichomes (a), the number of rosette leaves (b), the number of cauline leaves on the primary shoot (c), shoot architecture (d), cauline leaf heteroblasty (e), cauline leaf blade length : width ratios (f), and the number of leaves on each secondary inflorescence (g) in Columbia (Col-0), *spl qm*, *35S::SOC1*, *35S::FUL*, *35S::SOC1 spl qm*, and *35S::FUL spl qm*. Numbers in the upright corner of (d) indicate the number of plants showing the phenotype and the number of plants examined. (a–c), one-way ANOVA, $P < 0.05$, different letters above each graph represent significantly different groups. Bar, 1 cm. (f, g), two-way ANOVA, $P < 0.05$, different letters above each graph represent significantly different groups. Error bars represent SE.

elongated and tapered, lack petioles, are associated with elongated internodes and inflorescence buds, and produce trichomes predominantly on the abaxial surface. The unique developmental identity of cauline leaves was recently supported by a comparative analysis of vegetative and cauline leaf morphogenesis, which found specific patterns of cell division, expansion, and differentiation in cauline leaves (Le Gloanec *et al.*, 2024). The role of the miR156-*SPL* genetic module in regulating vegetative leaf identity (i.e. juvenile vs adult) has been well established (Wu & Poethig, 2006; Wu *et al.*, 2009; Xu *et al.*, 2016; He *et al.*, 2018).

However, whether *SPL* genes regulate the developmental identity of distinct leaf types remains to be determined. Here, we have demonstrated that *SPL* genes also function redundantly to promote cauline leaf development.

Recent work has shown that miR156-targeted *SPL* genes regulate leaf morphology through direct repression of *BLADE-ON-PETIOLE* genes during vegetative development (Hu *et al.*, 2023), which promote proximal-distal axis development by promoting petiole development and by prolonging the period of proliferative growth via regulation of cell cycle and cell wall

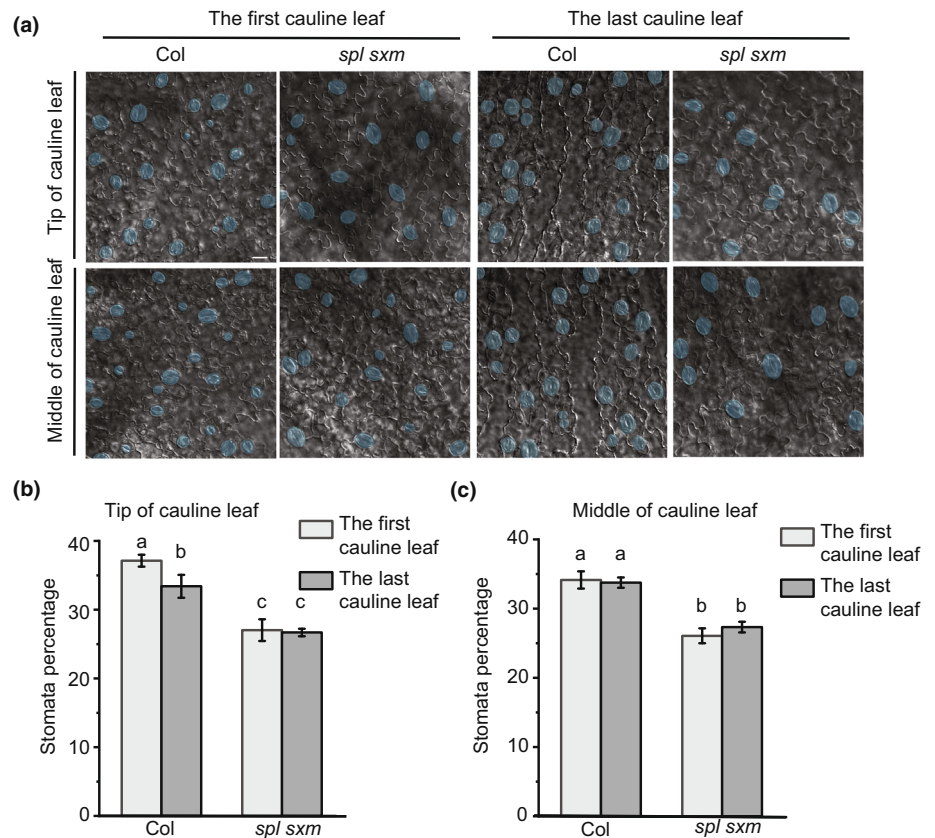


Fig. 8 SQUAMOSA PROMOTER BINDING PROTEIN-LIKE (*SPL*) genes promote the stomatal percentage of cauline leaves in *Arabidopsis*. (a) Abaxial epidermis of the tip and middle of the first and last cauline leaves of Columbia (Col-0) and *spl sextuple mutant* (*sxm*) with stomata artificially colored in blue by photoshop. Bar, 25 μm. (b, c) Stomatal percentage at the tip (b) and the middle (c) of the first and last cauline leaves in Col-0 and *spl sxm*. Shared letters above each bar indicate not significantly different groups, different letters above each bar indicate significantly different groups, $P < 0.05$, two way ANOVA (b, c). Cauline leaves were analyzed at 3–4 mm blade length. Error bars represent SE.

genetic networks (Tang *et al.*, 2023; Li *et al.*, 2024). The rounder leaves with extended petioles formed in *spl* mutant plants suggest *SPL* transcription factors regulate similar downstream targets during cauline leaf development. However, the unique cellular dynamics reported in cauline leaves relative to rosette leaves (Le Gloanec *et al.*, 2024) indicates either that the downstream networks have been modified or that additional morphogenetic factors are at play during cauline leaf development. As is the case in cauline leaves, *SPL9* appears to be a critical regulator of cauline leaf development (Fig. S1), although considerable genetic redundancy exists in the regulation of both vegetative and cauline leaf identities by members of the *SPL* family.

Cauline leaves represent an intermediate developmental phase between vegetative (rosette leaf) and reproductive (flower) development (Hempel *et al.*, 1997), and increased cauline leaf number, therefore, is a consequence of a delay in the transition to reproductive development. This increased number of cauline leaves in *spl* mutants is consistent with previous findings that miR156-targeted *SPL* transcription factors directly bind floral meristem specification genes *API* and *LFY* (Yamaguchi *et al.*, 2009, 2014). We observed a particularly strong increase in the number of leaves on *spl* secondary inflorescence shoots, suggesting that primary inflorescence and axillary meristems are differentially sensitive to *SPL* activity. The higher number of leaves on the secondary inflorescence branches in *soc1 ful* (Fig. 4d) relative to *spl sxm* (Fig. 1e) plants is likely due to additional regulation of *LFY* by *SOC1* and *FUL* independent of *SPLs* (Lee *et al.*, 2008).

SPLs are partially activated by floral activators

miR156 levels remain at low levels following vegetative development; however, miR156-targeted *SPLs* were upregulated upon floral induction. Furthermore, we observed an increase in *SPL* transcript accumulation following floral induction in *35S:MIM156* plants in which miR156 activity is blocked (Fig. 2). Taken together, these results indicate that *SPLs* regulate cauline leaf identity in a miR156-independent manner. Instead, *SPL* function during cauline leaf development appears largely dependent on transcriptional regulation by floral activator genes. The floral induction activators *SOC1*, *FUL*, *FD*, *CO*, *ADL24*, and *AGL42* do not promote *SPLs* during vegetative phase change, as mutations in these genes do not change the number of juvenile leaves (Figs 4a, 5a). However, they are competent to accelerate vegetative phase change when ectopically expressed, resulting in few juvenile leaves (Fig. 2b). Phenotypic and RT-qPCR analyses in floral activator mutants revealed that *SOC1* and *FUL* are the primary activators for *SPLs* during floral induction, while *FD*, *CO*, *AGL24*, and *AGL42* likely activate *SPLs* indirectly, probably through activating *SOC1* and *FUL*, as *SPL* genes were downregulated to similar levels in the *soc1 ful* double mutant as in higher order mutants containing *soc1 ful* (Fig. 6b). Consistent with these observations, cauline leaf morphology and the number of leaves on each secondary inflorescence in higher order *soc1 ful* mutants were not more severe than those of the *soc1 ful* double mutant (Fig. 5). The ChIP-qPCR and promoter analysis showed

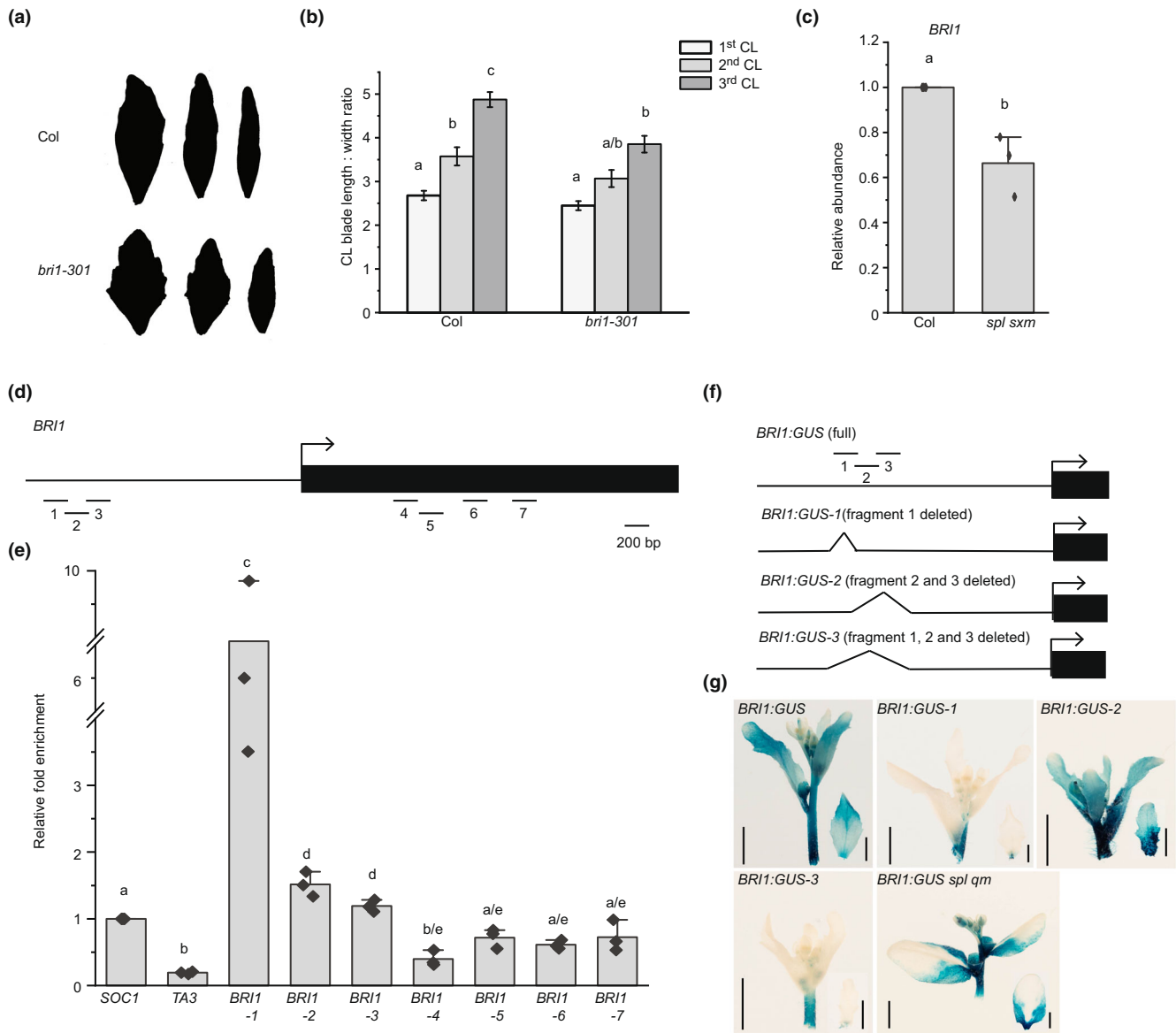


Fig. 9 SPL9 binds directly to BRASSINOSTEROID INSENSITIVE 1 (*BRI1*) to promote cauline leaf identity in *Arabidopsis*. (a, b) Cauline leaf heteroblasty (a) and cauline leaf blade length : width ratios of Columbia (Col-0) and *bri1-301* (b). (c) Reverse transcription quantitative polymerase chain reaction (RT-qPCR) analysis of *BRI1* in Col-0 and *spl sxm* (c). (d) Schematic diagram of *BRI1* genomic DNA and fragments tested for SPL9 binding. (e) Chromatin immunoprecipitation followed by qPCR (ChIP-qPCR) analysis of SPL9 binding to *BRI1*. SUPPRESSOR OF OVEREXPRESSION OF CONSTANS1 (*SOC1*) is a direct target of SPL9 and its percentage of input relative to Col-0 was set to be 1, and fold enrichment in *BRI1* fragments was normalized to *SOC1*. (f) Schematic diagram of *BRI1* promoter with indication of regions removed. (g) Expression of β -glucuronidase (*GUS*) in cauline leaves driven by the full-length or truncated variants of the *BRI1* promoter. Different letters above each bar represent significantly different groups, $P < 0.05$, one-way ANOVA (c, e), two-way ANOVA (b). Bars, 3 cm. Error bars represent SE. SPL, SQUAMOSA PROMOTER BINDING PROTEIN-LIKE.

that *SOC1* and *FUL* activate *SPL9* and *SPL15* directly (Fig. 6c–g). Nevertheless, the number of cauline leaves on the primary inflorescence of *soc1 ful* was more than that of the *spl sxm* mutant, probably caused by the activation of *SPLs* as well as the master floral meristem identity genes *LFY* and *API* by *SOC1* and *FUL* (Lee *et al.*, 2008; Liu *et al.*, 2008; Balanzà *et al.*, 2014). Similarly, the *soc1 ful* double mutant has more leaves on its secondary inflorescence than *spl* mutants, likely due to insufficient activation of *SPLs* and *LFY/API*. Since significant levels of *SPLs*

remained in the *soc1 ful* double mutant and higher order mutants containing *soc1 ful*, our data suggest that *SPLs* are partially activated by *SOC1* and *FUL* during floral induction for the establishment of cauline leaf identity. Other factors that activate *SPLs* independent of miR516 during floral induction remain to be uncovered.

We observed a particularly strong increase in the number of cauline leaves on *spl* secondary inflorescence shoots, suggesting that primary inflorescence and axillary meristems are

differentially sensitive to SPL activity. As secondary shoots continue to produce cauline leaves following the conversion of the primary inflorescence shoot to reproductive development, our results also suggest that the reproductive transition is regulated semi-independently across the shoot. This would be consistent with studies of vegetative phase change, which have shown that leaf identity is regulated independently of the SAM (Orkiszewski & Poethig, 2000) and that vegetative buds are able to maintain discrete identities in long-lived woody species (Bassiri *et al.*, 1992).

Even in the strong *spl sxm*, we did not observe any instances of aerial rosette formation, in which axillary meristems are converted to a vegetative state and entire rosettes initiate at elongated internodes. Aerial rosette formation is associated with enhanced activity of the floral repressors FLC and TFL1 (Grbić & Bleecker, 1996; Ratcliffe *et al.*, 1998; Poduska *et al.*, 2003). This supports the argument that *SPL* genes play only a minor role in the transition to inflorescence identity in *Arabidopsis* (Zhao *et al.*, 2023; Poethig & Fouracre, 2024), although additional *SPL* genes beyond *SPL2/9/10/11/13/15* may also function redundantly to promote inflorescence development in axillary meristems.

Stomata density may be a heteroblastic leaf trait

Previous reports have shown that suppression of *SPL* activity leads to lower rates of stomatal initiation in leaves of potato (Bhogale *et al.*, 2014) and tobacco (Feng *et al.*, 2016). Furthermore, cauline leaves have been shown to have a higher stomatal percentage than rosette leaves (Haus *et al.*, 2018; Ding *et al.*, 2023). This suggests that increased stomatal index may have been an overlooked element of heteroblastic development. Consistent with this notion, we found that *spl sxm* cauline leaves have a lower stomatal percentage than WT plants (Fig. 8). Conversely, Li *et al.* reported a higher stomatal percentage in the *spl9 spl15* mutant relative to WT (Li *et al.*, 2024), although in this instance leaves were surveyed at a much earlier developmental stage before full maturity. The exact role of the miR156/*SPL* module in stomatal development remains to be determined, although it is likely to include input from downstream cell proliferation pathways as stomata initiate at different rates across the leaf basipetal axis (Le Gloanec *et al.*, 2024; Li *et al.*, 2024). As overall rates of stomatal conductance were found to be the same between juvenile and adult *Arabidopsis* leaves (Lawrence *et al.*, 2020), the functional significance of stomata regulation by miR156/*SPL* in cauline leaves remains to be discovered.

BR signaling is involved in establishing cauline leaf identity

Brassinosteroids are important plant hormones that regulate various developmental processes, including root and shoot growth, vascular differentiation, pollen development, and seed formation (Ackerman-Lavert & Savaldi-Goldstein, 2020; Kim & Russinova, 2020; Oh *et al.*, 2020; Shi *et al.*, 2022). Brassinosteroids promote plant growth by enhancing cell expansion and proliferation, with their interaction with auxin playing a significant

role in shaping leaf morphology (Oh *et al.*, 2020; Xiong *et al.*, 2021). The perception of BRs begins with their binding to the receptor kinase BRI1 and its coreceptor, BRI1-Associated Kinase 1 (BAK1), initiating a signaling cascade that activates the transcription factor BZR1 and other downstream BR-responsive genes (Li & Chory, 1997; Wang *et al.*, 2002). BRASSINOSTEROID INSENSITIVE 1 is expressed in elongating and differentiating tissues, including the petioles and central veins of rosette and cauline leaves, and the spatial and temporal expression of *BRI1* is tightly regulated, with its distribution affecting BR sensitivity and signaling in specific tissues (Zhou *et al.*, 2004; Hategan *et al.*, 2014). Our results showed that *BRI1* and miR156-targeted *SPLs* are co-expressed in cauline leaves. *SPL9* directly binds to the promoter of *BRI1*, and mutations in *SPLs* lead to reduced expression of *BRI1* at the distal regions of cauline leaves. This highlights the critical role of BRs in cauline leaf development. Although the cauline leaf phenotype of *bri1-301* is milder than that of the higher order *spl* mutants, it suggests that miR156-targeted *SPLs* also regulate additional downstream targets to establish cauline leaf identity. These findings, together with previous studies showing that BR stabilizes *SPL9* and that BRI1 regulates *SPL9*, *SPL10*, and *SPL15*, suggest a feedforward loop between BRs and *SPL9* activity (Wang *et al.*, 2021; Zhou *et al.*, 2023). In this model, the upregulation of *SPLs* leads to the upregulation of *BRI1*, which stabilizes *SPLs* and further amplifies BR signaling and *SPL* activity. In combination with findings elsewhere, our results suggest that the BR and *SPL* pathways are integrated to regulate the identity of multiple leaf types.

Acknowledgements

We thank George Coupland, Scott Poethig, Jia Li, and ABRC for seeds. This work was supported by a grant from the National Science Foundation (IOS 1947274) to MX. JF is supported by a University Research Fellowship from the Royal Society (URF/R1/221069).

Competing interests

None declared.

Author contributions

DM and MX designed the research. DM, LD, QZ, YL, TH and MX performed the research and analyzed the data. DM, JF and MX wrote the paper. All authors read the paper.

ORCID

Liren Du  <https://orcid.org/0000-0003-1194-5942>
Jim P. Fouracre  <https://orcid.org/0000-0003-0049-3047>
Tieqiang Hu  <https://orcid.org/0000-0003-3088-1796>
Yifei Liao  <https://orcid.org/0000-0003-0629-5084>
Darren Manuela  <https://orcid.org/0009-0005-0886-5089>
Mingli Xu  <https://orcid.org/0000-0001-7997-573X>

Data availability

The data that support the findings of this study are available in this paper and in the [Supporting Information](#) files. Further inquiries can be directed to the corresponding authors.

References

- Ackerman-Lavert M, Savaldi-Goldstein S. 2020. Growth models from a brassinosteroid perspective. *Current Opinion in Plant Biology* 53: 90–97.
- Aryal B, Shinohara W, Honjo MN, Kudoh H. 2018. Genetic differentiation in cauline-leaf-specific wettability of a rosette-forming perennial *Arabidopsis* from two contrasting montane habitats. *Annals of Botany* 121: 1351–1360.
- Balanà V, Martínez-Fernández I, Ferrándiz C. 2014. Sequential action of FRUITFULL as a modulator of the activity of the floral regulators SVP and SOC1. *Journal of Experimental Botany* 65: 1193–1203.
- Balanà V, Martínez-Fernández I, Sato S, Yanofsky MF, Kaufmann K, Angenent GC, Bemer M, Ferrándiz C. 2018. Genetic control of meristem arrest and life span in *Arabidopsis* by a FRUITFULL-APETALA2 pathway. *Nature Communications* 9: 565.
- Bassiri A, Irish EE, Poethig RS. 1992. Heterochronic effects of Teopod 2 on the growth and photosensitivity of the maize shoot. *Plant Cell* 4: 497–504.
- Bhogale S, Mahajan AS, Natarajan B, Rajabhoj M, Thulasiram HV, Banerjee AK. 2014. MicroRNA156: a potential graft-transmissible microRNA that modulates plant architecture and tuberization in *Solanum tuberosum* ssp. andigena. *Plant Physiology* 164: 1011–1027.
- Blázquez MA, Soowal LN, Lee I, Weigel D. 1997. LEAFY expression and flower initiation in *Arabidopsis*. *Development* 124: 3835–3844.
- Borner R, Kampmann G, Chandler J, Gleissner R, Wisman E, Apel K, Melzer S. 2000. A MADS domain gene involved in the transition to flowering in *Arabidopsis*. *The Plant Journal* 24: 591–599.
- Busch MA, Bomblies K, Weigel D. 1999. Activation of a floral homeotic gene in *Arabidopsis*. *Science* 285: 585–587.
- Cho LH, Yoon J, An G. 2017. The control of flowering time by environmental factors. *The Plant Journal* 90: 708–719.
- Clough SJ, Bent AF. 1998. Floral dip: a simplified method for *Agrobacterium*-mediated transformation of *Arabidopsis thaliana*. *The Plant Journal* 16: 735–743.
- Ding M, Zhu Y, Kinoshita T. 2023. Stomatal properties of *Arabidopsis* cauline and rice flag leaves and their contributions to seed production and grain yield. *Journal of Experimental Botany* 74: 1957–1973.
- Doody E, Zha Y, He J, Poethig RS. 2022. The genetic basis of natural variation in the timing of vegetative phase change in *Arabidopsis thaliana*. *Development* 149: 4587.
- Feng S, Xu Y, Guo C, Zheng J, Zhou B, Zhang Y, Ding Y, Zhang L, Zhu Z, Wang H *et al.* 2016. Modulation of miR156 to identify traits associated with vegetative phase change in tobacco (*Nicotiana tabacum*). *Journal of Experimental Botany* 67: 1493–1504.
- Fouracre JP, Poethig RS. 2019. Role for the shoot apical meristem in the specification of juvenile leaf identity in *Arabidopsis*. *Proceedings of the National Academy of Sciences, USA* 116: 10168–10177.
- Freytes SN, Canelo M, Cerdán PD. 2021. Regulation of flowering time: when and where? *Current Opinion in Plant Biology* 63: 102049.
- Grbić B, Bleecker AB. 1996. An altered body plan is conferred on *Arabidopsis* plants carrying dominant alleles of two genes. *Development* 122: 2395–2403.
- Hategan L, Godza B, Kozma-Bognar L, Bishop GJ, Szekeres M. 2014. Differential expression of the brassinosteroid receptor-encoding BRI1 gene in *Arabidopsis*. *Planta* 239: 989–1001.
- Haus MJ, Li M, Chitwood DH, Jacobs TW. 2018. Long-distance and trans-generational stomatal patterning by CO(2) across *Arabidopsis* organs. *Frontiers in Plant Science* 9: 1714.
- He J, Xu M, Willmann MR, McCormick K, Hu T, Yang L, Starker CG, Voytas DF, Meyers BC, Poethig RS. 2018. Threshold-dependent repression of SPL gene expression by miR156/miR157 controls vegetative phase change in *Arabidopsis thaliana*. *PLoS Genetics* 14: e1007337.
- Hempel FD, Weigel D, Mandel MA, Ditta G, Zambryski PC, Feldman LJ, Yanofsky MF. 1997. Floral determination and expression of floral regulatory genes in *Arabidopsis*. *Development* 124: 3845–3853.
- Hu T, Manuela D, Xu M. 2023. SQUAMOSA PROMOTER BINDING PROTEIN-LIKE 9 and 13 repress BLADE-ON-PETIOLE 1 and 2 directly to promote adult leaf morphology in *Arabidopsis*. *Journal of Experimental Botany* 74: 1926–1939.
- Kim EJ, Russinova E. 2020. Brassinosteroid signalling. *Current Biology* 30: R294–r298.
- Lawrence EH, Springer CJ, Helliker BR, Poethig RS. 2020. miR156-mediated changes in leaf composition lead to altered photosynthetic traits during vegetative phase change. *New Phytologist* 231: 1008–1022.
- Lawrence EH, Springer CJ, Helliker BR, Poethig RS. 2021. MicroRNA156-mediated changes in leaf composition lead to altered photosynthetic traits during vegetative phase change. *New Phytologist* 231: 1008–1022.
- Le Gloanec C, Gómez-Felipe A, Alimchandani V, Branchini E, Bauer A, Routier-Kierzkowska AL, Kierzkowski D. 2024. Modulation of cell differentiation and growth underlies the shift from bud protection to light capture in cauline leaves. *Plant Physiology* 196: 1214–1230.
- Lee J, Lee I. 2010. Regulation and function of SOC1, a flowering pathway integrator. *Journal of Experimental Botany* 61: 2247–2254.
- Lee J, Oh M, Park H, Lee I. 2008. SOC1 translocated to the nucleus by interaction with AGL24 directly regulates leafy. *The Plant Journal* 55: 832–843.
- Li J, Chory J. 1997. A putative leucine-rich repeat receptor kinase involved in brassinosteroid signal transduction. *Cell* 90: 929–938.
- Li XM, Jenke H, Strauss S, Bazakos C, Mosca G, Lymbouridou R, Kierzkowski D, Neumann U, Naik P, Huijser P *et al.* 2024. Cell-cycle-linked growth reprogramming encodes developmental time into leaf morphogenesis. *Current Biology* 34: 541–556.
- Liu C, Chen H, Er HL, Soo HM, Kumar PP, Han JH, Liou YC, Yu H. 2008. Direct interaction of AGL24 and SOC1 integrates flowering signals in *Arabidopsis*. *Development* 135: 1481–1491.
- Manuela D, Xu M. 2024. Aintegumenta and redundant Aintegumenta-Like6 are required for bract outgrowth in *Arabidopsis*. *Journal of Experimental Botany* 75: 3920–3931.
- van Mourik H, Chen P, Smaczniak C, Boeren S, Kaufmann K, Bemer M, Angenent GC, Muino JM. 2023. Dual specificity and target gene selection by the MADS-domain protein FRUITFULL. *Nature Plants* 9: 473–485.
- Oh MH, Honey SH, Tax FE. 2020. The control of cell expansion, cell division, and vascular development by brassinosteroids: a historical perspective. *International Journal of Molecular Sciences* 21: 1569.
- Orkiszewski JA, Poethig RS. 2000. Phase identity of the maize leaf is determined after leaf initiation. *Proceedings of the National Academy of Sciences, USA* 97: 10631–10636.
- Pabón-Mora N, Sharma B, Holappa LD, Kramer EM, Litt A. 2013. The Aquilegia FRUITFULL-like genes play key roles in leaf morphogenesis and inflorescence development. *The Plant Journal* 74: 197–212.
- Patharkar OR. 2019. Quantification of cauline leaf abscission in response to plant pathogens. *Methods in Molecular Biology* 1991: 127–139.
- Patharkar OR, Gassmann W, Walker JC. 2017. Leaf shedding as an anti-bacterial defense in *Arabidopsis* cauline leaves. *PLoS Genetics* 13: e1007132.
- Patharkar OR, Walker JC. 2016. Core mechanisms regulating developmentally timed and environmentally triggered abscission. *Plant Physiology* 172: 510–520.
- Poduska B, Humphrey T, Redweik A, Grbić V. 2003. The synergistic activation of FLOWERING LOCUS C by FRIGIDA and a new flowering gene AERIAL ROSETTE 1 underlies a novel morphology in *Arabidopsis*. *Genetics* 163: 1457–1465.
- Poethig RS, Fouracre J. 2024. Temporal regulation of vegetative phase change in plants. *Developmental Cell* 59: 4–19.
- Ratcliffe OJ, Amaya I, Vincent CA, Rothstein S, Carpenter R, Coen ES, Bradley DJ. 1998. A common mechanism controls the life cycle and architecture of plants. *Development* 125: 1609–1615.

- Samach A, Onouchi H, Gold SE, Ditta GS, Schwarz-Sommer Z, Yanofsky MF, Coupland G. 2000. Distinct roles of CONSTANS target genes in reproductive development of *Arabidopsis*. *Science* 288: 1613–1616.
- Schmid M, Uhlenhaut NH, Godard F, Demar M, Bressan R, Weigel D, Lohmann JU. 2003. Dissection of floral induction pathways using global expression analysis. *Development* 130: 6001–6012.
- Shi H, Li X, Lv M, Li J. 2022. BES1/BZR1 family transcription factors regulate plant development via brassinosteroid-dependent and independent pathways. *International Journal of Molecular Sciences* 23: 532.
- Shikata M, Koyama T, Mitsuda N, Ohme-Takagi M. 2009. *Arabidopsis* SBP-box genes SPL10, SPL11 and SPL2 control morphological change in association with shoot maturation in the reproductive phase. *Plant & Cell Physiology* 50: 2133–2145.
- Tang HB, Wang J, Wang L, Shang GD, Xu ZG, Mai YX, Liu YT, Zhang TQ, Wang JW. 2023. Anisotropic cell growth at the leaf base promotes age-related changes in leaf shape in *Arabidopsis thaliana*. *Plant Cell* 35: 1386–1407.
- Tao Z, Shen L, Liu C, Liu L, Yan Y, Yu H. 2012. Genome-wide identification of SOC1 and SVP targets during the floral transition in *Arabidopsis*. *The Plant Journal* 70: 549–561.
- Telfer A, Bollman KM, Poethig RS. 1997. Phase change and the regulation of trichome distribution in *Arabidopsis thaliana*. *Development* 124: 645–654.
- Torti S, Fornara F. 2012. AGL24 acts in concert with SOC1 and FUL during *Arabidopsis* floral transition. *Plant Signaling & Behavior* 7: 1251–1254.
- Torti S, Fornara F, Vincent C, Andrés F, Nordström K, Göbel U, Knoll D, Schoof H, Coupland G. 2012. Analysis of the *Arabidopsis* shoot meristem transcriptome during floral transition identifies distinct regulatory patterns and a leucine-rich repeat protein that promotes flowering. *Plant Cell* 24: 444–462.
- Wagner D, Sablowski RW, Meyerowitz EM. 1999. Transcriptional activation of APETALA1 by LEAFY. *Science* 285: 582–584.
- Wang JW, Czech B, Weigel D. 2009. miR156-regulated SPL transcription factors define an endogenous flowering pathway in *Arabidopsis thaliana*. *Cell* 138: 738–749.
- Wang L, Yu P, Lyu J, Hu Y, Han C, Bai MY, Fan M. 2021. BZR1 physically interacts with SPL9 to regulate the vegetative phase change and cell elongation in *Arabidopsis*. *International Journal of Molecular Sciences* 22: 158.
- Wang ZY, Nakano T, Gendron J, He J, Chen M, Vafeados D, Yang Y, Fujioka S, Yoshida S, Asami T *et al.* 2002. Nuclear-localized BZR1 mediates brassinosteroid-induced growth and feedback suppression of brassinosteroid biosynthesis. *Developmental Cell* 2: 505–513.
- Weber E, Gruetzner R, Werner S, Engler C, Marillonnet S. 2011. Assembly of designer TAL effectors by golden gate cloning. *PLoS ONE* 6: e19722.
- Weigel D, Alvarez J, Smyth DR, Yanofsky MF, Meyerowitz EM. 1992. LEAFY controls floral meristem identity in *Arabidopsis*. *Cell* 69: 843–859.
- Wigge PA, Kim MC, Jaeger KE, Busch W, Schmid M, Lohmann JU, Weigel D. 2005. Integration of spatial and temporal information during floral induction in *Arabidopsis*. *Science* 309: 1056–1059.
- Wu G, Park MY, Conway SR, Wang JW, Weigel D, Poethig RS. 2009. The sequential action of miR156 and miR172 regulates developmental timing in *Arabidopsis*. *Cell* 138: 750–759.
- Wu G, Poethig RS. 2006. Temporal regulation of shoot development in *Arabidopsis thaliana* by miR156 and its target SPL3. *Development* 133: 3539–3547.
- Xing H-L, Dong L, Wang Z-P, Zhang H-Y, Han C-Y, Liu B, Wang X-C, Chen Q-J. 2014. A CRISPR/Cas9 toolkit for multiplex genome editing in plants. *BMC Plant Biology* 14: 327.
- Xiong Y, Wu B, Du F, Guo X, Tian C, Hu J, Lü S, Long M, Zhang L, Wang Y *et al.* 2021. A crosstalk between auxin and brassinosteroid regulates leaf shape by modulating growth anisotropy. *Molecular Plant* 14: 949–962.
- Xu M, Hu T, Zhao J, Park MY, Earley KW, Wu G, Yang L, Poethig RS. 2016. Developmental functions of miR156-regulated SQUAMOSA PROMOTER BINDING PROTEIN-LIKE (SPL) genes in *Arabidopsis thaliana*. *PLoS Genetics* 12: e1006263.
- Yamaguchi A, Wu MF, Yang L, Wu G, Poethig RS, Wagner D. 2009. The microRNA-regulated SBP-Box transcription factor SPL3 is a direct upstream activator of LEAFY, FRUITFULL, and APETALA1. *Developmental Cell* 17: 268–278.
- Yamaguchi N, Winter CM, Wu MF, Kanno Y, Yamaguchi A, Seo M, Wagner D. 2014. Gibberellin acts positively then negatively to control onset of flower formation in *Arabidopsis*. *Science* 344: 638–641.
- Yang M, Jiao Y. 2016. Regulation of axillary meristem initiation by transcription factors and plant hormones. *Frontiers in Plant Science* 7: 489.
- Zhao J, Doody E, Poethig RS. 2023. Reproductive competence is regulated independently of vegetative phase change in *Arabidopsis thaliana*. *Current Biology* 33: 487–497.
- Zhou A, Wang H, Walker JC, Li J. 2004. BRL1, a leucine-rich repeat receptor-like protein kinase, is functionally redundant with BRI1 in regulating *Arabidopsis* brassinosteroid signaling. *The Plant Journal* 40: 399–409.
- Zhou B, Luo Q, Shen Y, Wei L, Song X, Liao H, Ni L, Shen T, Du X, Han J *et al.* 2023. Coordinated regulation of vegetative phase change by brassinosteroids and the age pathway in *Arabidopsis*. *Nature Communications* 14: 2608.

Supporting Information

Additional Supporting Information may be found online in the Supporting Information section at the end of the article.

Fig. S1 *sp1* single or double mutants and cauline leaf identity.

Fig. S2 Construction of the CRISPR/Cas9 mutant line *agl42*.

Fig. S3 LFY regulates cauline leaf number.

Fig. S4 Overexpression of flowering-time genes resulted in early flowering and early vegetative phase change.

Fig. S5 Expressing miR156 under floral activator gene promoters did not affect the number of cauline leaves on the primary inflorescence.

Fig. S6 *SOC1::SOC1-GFP* complemented the *soc1-2* mutant.

Fig. S7 Cauline leaf number was not significantly affected in *bri1-301*.

Table S1 Primers used for genotyping.

Table S2 Primers used for cloning.

Table S3 Primers used for RT-qPCR.

Table S4 Primers used for CHIP-qPCR.

Please note: Wiley is not responsible for the content or functionality of any Supporting Information supplied by the authors. Any queries (other than missing material) should be directed to the *New Phytologist* Central Office.

Disclaimer: The New Phytologist Foundation remains neutral with regard to jurisdictional claims in maps and in any institutional affiliations.